

DUDLEY KNOX LIBRARY
NAVAL POSTGRADUATE SCHOOL
MONTEREY, CALIFORNIA 93943-5002

NPS72-86-002

NAVAL POSTGRADUATE SCHOOL

Monterey, California



THESIS

SOLAR CELL CONCENTRATOR SYSTEM

by

Nevsan Sengil

December 1986

Thesis Advisor:

A. E. Fuhs

Approved for public release; distribution is unlimited.

Prepared for: Department of the Navy
Commander Space and Naval Warfare
System Command, SPAWAR-004-4
Washington, D.C. 20362-5100

T232244

NAVAL POSTGRADUATE SCHOOL
Monterey, California

Rear Admiral R.C. Austin
Superintendent

David Schradly
Provost

This thesis was prepared in conjunction with research supported in part by Commander Space and Naval Warfare Systems Command, SPAWAR-004-4, Washington, D.C.

Reproduction of all or part of this report is authorized.

REPORT DOCUMENTATION PAGE

1a REPORT SECURITY CLASSIFICATION UNCLASSIFIED			1b RESTRICTIVE MARKINGS		
2a SECURITY CLASSIFICATION AUTHORITY			3 DISTRIBUTION/AVAILABILITY OF REPORT Unlimited Distribution		
2b DECLASSIFICATION/DOWNGRADING SCHEDULE					
4 PERFORMING ORGANIZATION REPORT NUMBER(S) NPS72-86-002			5 MONITORING ORGANIZATION REPORT NUMBER(S)		
6a NAME OF PERFORMING ORGANIZATION Naval Postgraduate School		6b OFFICE SYMBOL (if applicable) Code 72		7a NAME OF MONITORING ORGANIZATION Commander Space and Naval Warfare Systems Command, Code SPAWAR-004-4	
6c ADDRESS (City, State, and ZIP Code) Monterey, CA 93943-5000			7b ADDRESS (City, State, and ZIP Code) Washington, D.C. 30363-5100		
8a NAME OF FUNDING/SPONSORING ORGANIZATION		8b OFFICE SYMBOL (if applicable) PDW 106-483		9 PROCUREMENT INSTRUMENT IDENTIFICATION NUMBER N4175686WR67571	
8c ADDRESS (City, State, and ZIP Code) Washington, D.C. 20363-5100			10 SOURCE OF FUNDING NUMBERS		
			PROGRAM ELEMENT NO	PROJECT NO	TASK NO
			WORK UNIT ACCESSION NO		
11 TITLE (Include Security Classification) SOLAR CELL CONCENTRATOR SYSTEM					
12 PERSONAL AUTHOR(S) Sengil, Nevshan					
13a TYPE OF REPORT Master's Thesis		13b TIME COVERED FROM TO		14 DATE OF REPORT (Year, Month, Day) 1986 December	
15 PAGE COUNT 53					
16 SUPPLEMENTARY NOTATION					
17 COSATI CODES			18 SUBJECT TERMS (Continue on reverse if necessary and identify by block number)		
FIELD	GROUP	SUB-GROUP	GaAs Concentrator Cell; Heat Pipe; Cell I-V Curves		
19 ABSTRACT (Continue on reverse if necessary and identify by block number)					
<p>If solar cells are exposed to charged particle radiation, efficiency decreases. Also solar cell efficiency is increased by concentrated solar light. A solar cell concentrator system includes shielding against particle radiation and provides concentrated solar light, with increased efficiency.</p> <p>A solar cell concentrator system was constructed using a GaAs solar cell. Using a heat pipe, heat was transferred to a radiator. Cell operating temperature was measured. At the operating temperature (77°C) and under concentrated solar light (Concentration Ratio ≈ 130) solar cell efficiency was measured. Observed efficiency was 18.18 ± 0.18 (%). These results were used to calculate the performance of an array, consisting of small concentrators. The performance of the concentrator array was compared with a conventional array, and demonstrated the higher efficiency advantages.</p>					
20 DISTRIBUTION/AVAILABILITY OF ABSTRACT <input checked="" type="checkbox"/> UNCLASSIFIED/UNLIMITED <input type="checkbox"/> SAME AS RPT <input type="checkbox"/> DTIC USERS			21 ABSTRACT SECURITY CLASSIFICATION UNCLASSIFIED		
22a NAME OF RESPONSIBLE INDIVIDUAL Allen E. Fuhs			22b TELEPHONE (Include Area Code) 408-646-2948		22c OFFICE SYMBOL Code 72

Approved for public release; distribution is unlimited

Solar Cell Concentrator System

by

Neusan Sengil
Lieutenant J.G., Turkish Navy
B.S., Turkish Naval Academy

Submitted in partial fulfillment of the
requirements for the degree of

MASTER OF SCIENCE IN ENGINEERING SCIENCE

from the

NAVAL POSTGRADUATE SCHOOL
December 1986

A

ABSTRACT

If solar cells are exposed to charged particle radiation , efficiency decreases. Also solar cell efficiency is increased by concentrated solar light. A solar cell concentrator system includes shielding against particle radiation and provides concentrated solar light, with increased efficiency.

A solar cell concentrator system was constructed using a GaAs solar cell. Using a heat pipe, heat was transferred to a radiator. Cell operating temperature was measured. At the operating temperature (77°C) and under concentrated solar light (Concentration Ratio $\cong 130$) solar cell efficiency was measured. Observed efficiency was 18.18 ± 0.18 (%). These results were used to calculate the performance of an array, consisting of small concentrators. The performance of the concentrator array was compared with a conventional array, and demonstrated the higher efficiency advantages.

TABLE OF CONTENTS

I.	INTRODUCTION -----	6
II.	TEST SYSTEM -----	8
A.	SOFTWARE -----	8
1.	Software E1 -----	8
2.	Software ECON -----	9
3.	Software LOGS -----	10
B.	EQUIPMENT SET-UP -----	10
III.	UNIT CONCENTRATOR SYSTEM -----	12
A.	EFFECT OF CONCENTRATION -----	12
B.	SOLUTION TO HEAT PROBLEM -----	13
IV.	DISCUSSION OF TEST RESULTS -----	18
A.	CONCENTRATOR ARRAY PERFORMANCE -----	18
B.	ERROR ANALYSIS -----	18
V.	RECOMMENDATIONS -----	20
	APPENDIX A : CELL CURRENT-VOLTAGE CURVES -----	21
	APPENDIX B : SOLUTION TO DIFFERENTIAL EQUATION -----	46
	LIST OF REFERENCES -----	49
	BIBLIOGRAPHY -----	50
	INITIAL DISTRIBUTION LIST -----	51

ACKNOWLEDGEMENT

The author wishes to thank Distinguished Professor A.E. Fuhs for his guidance in the preparation of this theses. Additionally the author wishes to thank Mr. T. McCord for fabricating the concentrator cell assembly.

I. INTRODUCTION

As the missions for space vehicles become more demanding, additional electrical power is needed from solar cell arrays. That means bigger, lighter, more efficient solar cells are required; further, these arrays must operate over longer periods of time. One way of meeting this demand is to build a solar cell concentrator system. A need exists for a solar cell array which consists of modular concentrator systems. According to the NASA Lewis Research Center studies, the economical region for unit concentrator system is between X20 and X200(AM0). More detail is given by Dennis [Ref. 1:p. 7]. In this thesis, $C \cong 130(AM0)$ was chosen as a concentration level. A decision was made to use an reflector type concentrator. Because of the reflection losses, it is decided to reflect the light directly just one time on to the solar cell. In order to avoid the shadow of the cell on the mirror, an off-axis type reflector was selected for this particular design. To transfer the heat from the solar cell to a radiator, a heat pipe was purchased. The radiator is located on the back side of the solar cell array. In order to protect the cell from the flux of charged particles due to the space environment, a shield was added to the unit system. A combination of theory and experiments gave the overall total efficiency of this kind of concentrator solar cell array.

Research was conducted at Naval Postgraduate School Solar Cell Laboratory. This laboratory already had a wide variety of instruments useful for solar cell research. All these devices are described in detail

in Gold [Ref. 2:p. 10]. To build the concentrator system, an off-axis parabolic mirror (Melles Griot Part Number 02POA027), a Noren 3 Watts Copper-Water Heat-Pipe, and 6 Ga-As Concentrator Solar Cells (Applied Solar Energy Corporation) were purchased. A picture of the solar cell is in Figure 1. The active area is the dark circle which has a diameter of 4 mm; please note the metric scale. Later a radiation shield for the system was constructed.

Chapter Two is an explanation of the software programs and measurement equipment which were used to obtain solar cell performance. The third chapter discusses the heat problem and its solution. Also Chapter Three gives the operating temperature of the concentrator system. Chapter Four is a discussion of test results and possible errors. Recommendations are included in Chapter Five.

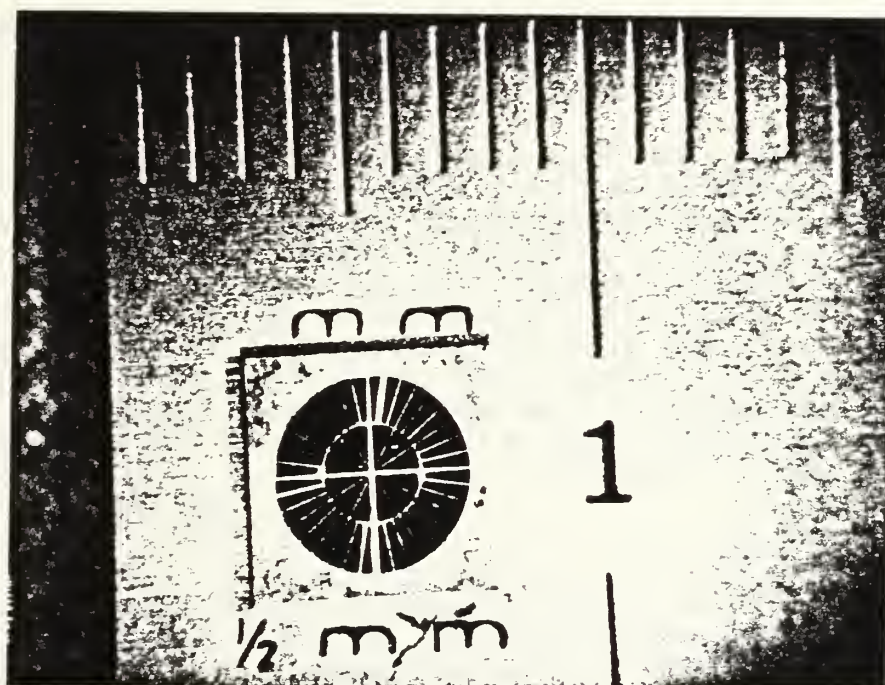


Figure 1. Photograph of the Concentrator Solar Cell

II. TEST SYSTEM

A. SOFTWARE

In order to derive the Current-Voltage curves known as the I-V curves and other characteristics of solar cells for X1 and X130(AM0), two different software programs were written. Software program E1 was written for unconcentrated solar light while software program ECON was written for concentrated solar light. Both programs are part of a computer controlled measurement system, and both programs are written in IBM Basica Language.

A third software program was written for conversion of linear I-V curves to logarithmic scale. With a logarithmic scale, the observer can easily compare the I-V curves for different concentration levels. The data are collected automatically under computer control and are either stored on a diskette for later computation or processed immediately and displayed on a hard copy plotter. The desired program is loaded into computer from hard disk, the cell connected with test block and the test is started by typing E1.BASICA or ECON.BASICA. From this point on, the interactive program asks for choices of user and displays the messages and data on monitor screen.

1. Software E1

This program is used to measure the cell conversion efficiency and I-V curves at X1(AM0). In this measurement, the solar cell to be tested is connected to test prows. A Kratos solar light simulator is set to AM0 (1353 W/m^2) based upon measured I_{sc} (Short circuit current) for

calibrated GaAs cell. Next the computer applies a short circuit condition to the cell and measures both the current in the circuit and the voltage directly across the solar cell. Due to the series resistance in the cell, the self bias of the cell is slightly forward. The computer decreases the voltage applied to the cell in steps of approximately 2mV and records the voltage at each step until it gets the first negative value. The short circuit current is computed by interpolating between currents obtained at slightly negative and slightly positive voltages. The computer then increases the applied voltage in positive 2mV steps recording current and voltage at each point. The open circuit voltage (V_{OC}) is found by interpolating between the voltages obtained at slightly positive and slightly negative currents.

The computer calculates the power at each data point and searches for the maximum power (P_{max}). Fill Factor (FF) is determined from

$$FF = \frac{P_{max}}{I_{SC} * V_{OC}} \quad (1)$$

The voltage and current at maximum power point gives I_{max} and V_{max} values. The computer plots the complete I-V curve using a HP 7475A plotter and displays the relevant parameters including I_{SC} , V_{OC} , P_{max} , V_{max} , I_{max} , efficiency(η), FF, date, concentration level (C) and cell name. Also the data are recorded to the user's floppy disk.

2. Software ECON

This software is slightly differ from E1. Measurements are made under concentrated solar light. The concentration ratio is determined by measuring I_{SC} under concentrated light and I_{SC0} of the same cell under one sun light. The concentration ratio is then given by

$$C = \frac{I_{SC}}{I_{SCO}} \quad (2)$$

The concentration ratio is changed by controlling the distance of solar cell to the solar light source. The efficiency is computed from

$$\eta = \frac{P_{max} * I_{SCO}}{P_i * A_C * I_{SC}} \quad (3)$$

In this equation, A_C represents the cell surface area, and P_i is the power of the X1(AM0) sun light for unit area.

3. Software LOGS

This particular software is used to convert the linear scale I-V curve plots to logarithmic scales. By using this software, an observer can easily see the effect of concentrated solar light on the solar cell FF, I_{SC} and V_{OC} .

B. EQUIPMENT SET-UP

A high concentration test facility that provides concentrated solar light at variable intensities (up to X200 AM0) for a solar image 0.5 cm. in diameter was developed. The Kratos 2500 light source is used as a solar light simulator. The temperature controlled test block is specially designed to accomodate solar cells with different shape and dimensions. For details, see Gold [Ref. 2:p. 16]. The test block provides three things: first holds the cell; second, provides electrical connections; and, third, provides a heat sink for the solar cell. A thermocouple is mounted to the test block very near to the cell to measure the cell temperature. The temperature is controlled by the cooling water. Cooling water is obtained from a CH/P temperature control circuit at fixed flow rate. One IBM digital/analog (D/A) converter is assigned to measure the

cell output voltage. Current is measured by a HP-3478A multimeter. The sink power supply is a combination of HP-59501B and HP-6825A; these units function as a variable impedance. The computer is an IBM-PC/XT, with a 10 MB harddisk. An HP-7475A is used as a plotter. More details are given by Gold [Ref. 2:pp. 20-26].

III. UNIT CONCENTRATOR SYSTEM

A. EFFECT OF CONCENTRATION

Using software E1, GaAs concentrator cells were tested. The temperature was set to 28⁰ C. Results are summarized in Table 3-1.

TABLE 3-1						
MEASURED CELL EFFICIENCY AT T=28 ⁰ C AND C=1						
CELL NAME	CELL1	CELL2	CELL3	CELL4	CELL5	CELL6
EFFICIENCY	16.3	16.9	16.5	16.6	16.6	17.2

The mean efficiencies of these cells is $\bar{\eta} = 16.68$ with a standard deviation ± 0.32 . I-V curves of these cells are included in Appendix A. Using software ECON, the second test of the cell with concentrated flux were obtained. Temperature was set to 28⁰ C, and the concentration of light was derived from Equation (2). I_{sc0} is the cell's short circuit current for X1(AM0) at the same temperature. For more details, see James [Ref. 3:p. 24]. Table 3-2 contains these cells and their efficiencies.

TABLE 3-2						
MEASURED CELL EFFICIENCIES AT T=28 ⁰ C AND C \approx 130						
CELL NAME	CELL1	CELL2	CELL3	CELL4	CELL5	CELL6
EFFICIENCY	20.26	19.77	19.41	19.91	19.80	19.99

The mean efficiencies of these cells is $\bar{\eta} = 19.82$ with a standard deviation ± 0.23 . I-V curves of these cells are included in Appendix A.

Because of the concentration of light, efficiencies are improved. The I-V curves of the same cell under different concentration levels are plotted on the same plot with a logarithmic scale. These plots are included in Appendix A.

B. SOLUTION TO HEAT PROBLEM

The efficiency increase because of the concentration of sun light is an advantage of the concentrator system. But at the same time, the heat collected on the solar cell increases considerably. The energy carried by photons which cannot be converted to electric energy is converted to heat. In space the heat is transferred by radiation. If energy collected on the solar cell is not removed and radiated to space, the solar cell becomes very hot. If we assume both sides of the cell radiates to space ($T_s = 0^\circ \text{ K}$) as a black body under a concentration level $X130(\text{AM}0)$, the temperature of solar cell will reach to $T_c = 778^\circ \text{ C}$ according to equation

$$T_c^4 = \frac{P_i * C * A_c}{\sigma * A_r} \quad (4)$$

σ is the Stephan-Boltzman constant and is equal to an experimental value of $5.73 * 10^{-8} \text{ W}/(\text{m}^2 \cdot \text{K}^4)$. A_r is the total radiation area and, in this case, equals

$$A_r = 2 * A_c \quad (5)$$

It is a necessity to provide an operating temperature for the solar cell which cannot damage the cell. A safe operating temperature can be achieved by carrying the excessive heat from the solar cell to a large radiation area. In this particular design, heat is carried by a heat pipe to the array back surface and radiated to space. At $C = 130$ and $\text{AM}0$ conditions, the solar energy which is incident on the solar cell is

$$W_i = C * P_i * A_c \quad (6)$$

$$W_i = 130 * 0.1353 * 0.1256 \quad (7)$$

$$W_i = 2.21 \text{ Watts} \quad (8)$$

The cross section area of paraboloid mirror for a $C = 130$ must be equal to

$$A_m = C * A_c \quad (9)$$

$$A_m = 16.33 \text{ cm}^2. \quad (10)$$

According to the Melles-Griot [Ref. 4:p. 193], the reflection coefficient for the mirror used in these experiments is $\rho = 0.8$ for solar light. That means the cross sectional area of the mirror for $C = 130$ should be equal to

$$A_{mr} = A_m / \rho \quad (11)$$

$$A_{mr} = 20.41 \text{ cm}^2 \quad (12)$$

If small concentrator systems are assembled to build a bigger solar array, the packaging factor (P.F.) should be calculated. As a special case orthogonal close packing is considered. In this case, $P.F. \cong 0.907$. More detail is provided in Appendix B. Because of the $P.F. = 0.907$, every unit has a radiation area of

$$A_r = A_{mr} / P.F. \quad (13)$$

$$A_r = 22.5 \text{ cm}^2. \quad (14)$$

The radial variation in temperature in the thermally-radiating disc located on the back surface of the mirror is analyzed in Appendix B. The radiation efficiency of the array back surface is sufficient to allow an assumption that $\Omega = 1$ as a very good approximation. That means the back surface radiates as if the temperature were uniform and equal to the T_i .

Emittance of radiator is taken $\epsilon = 0.96$ for an oil paint. It is assumed the radiator radiates to $T_s = 0$ K. Actually $T_s \cong 3$ K. With these assumptions T_i can be calculated from,

$$T_i^4 = \frac{P_i * (1 - \bar{\eta})}{\sigma * \epsilon * A_r * \Omega} \quad (15)$$

Figure 2 is the plot of T_i vs. $\bar{\eta}$. From Equation (15), T_i is a function of $\bar{\eta}$. But the same time $\bar{\eta}$ is a function of T_{op} (Cell operating temperature). Figure 3 is a plot of T_{op} vs. $\bar{\eta}$. T_{op} is calculated from

$$T_{op} = T_i + \Delta T \quad (16)$$

Where ΔT is the temperature difference between the solar cell and the radiator. Equation (15) must be solved by iteration since $\bar{\eta}$ is a function of T_{op} by Equation (16), and of T_i . Assume $T_{op} = 28^\circ\text{C}$ and $C = 130$; $\bar{\eta}$ is taken as 0.20. Then T_i is obtained from Figure 2 for $\bar{\eta} = 0.20$. Figure 3 gives an $\bar{\eta}$ for the T_{op} which is calculated from Equation (16). This $\bar{\eta}$ gives a new T_i in Figure 2. This process is repeated until η is the same value in Figure 2 and Figure 3. The condenser section of the heat pipe is put into water which serves as the heat sink. The temperature of the heat sink is taken equal to T_i . Next, the evaporator section of heat pipe is attached to the solar cell. The solar cell is exposed to light. The heat pipe body is insulated by an insulator material in order to prevent further heat loss by convection to the air. Also the heat pipe is placed horizontal in order to compensate for the effect of gravity. ΔT is found by experiments to equal to 2°C . The heat sink and the heat pipe were photographed in Figure 4. After one series of repetition of these measurements, efficiency is found to be $\bar{\eta} \cong 18.18$. Operating temperature was measured using Chromel-Alumel thermocouple and was found to be

$T_{op}=77^{\circ}\text{C}$. The I-V curves of solar cells are in Appendix A. Table 3-3 gives the cells efficiencies at $T_{op}=77^{\circ}\text{C}$ and $C\cong 130$.

TABLE 3-3						
MEASURED CELL EFFICIENCIES AT $T=77^{\circ}\text{C}$ AND $C\cong 130$						
CELL NAME	CELL1	CELL2	CELL3	CELL4	CELL5	CELL6
EFFICIENCY	18.25	18.01	18.24	18.47	18.10	17.99

The mean efficiencies of these cells is 18.18 with a standard deviation ± 0.18 .

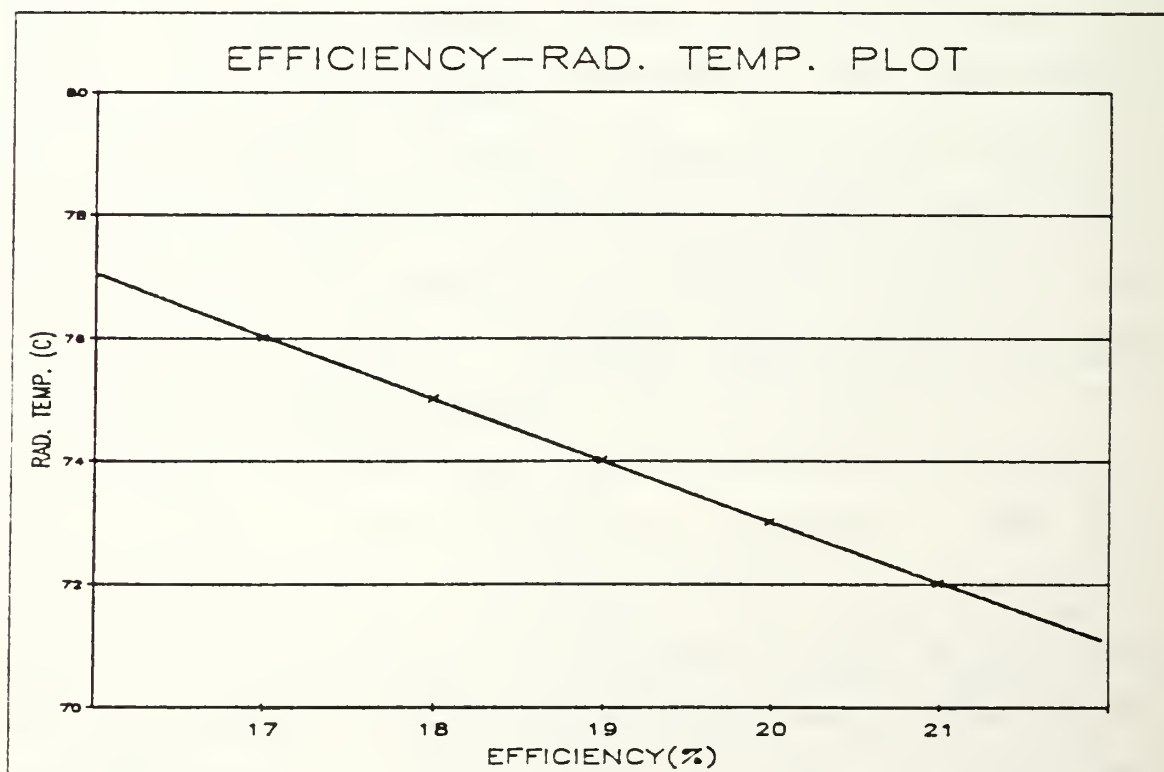


Figure 2 . Radiator Temperature as a Function of Cell Efficiency

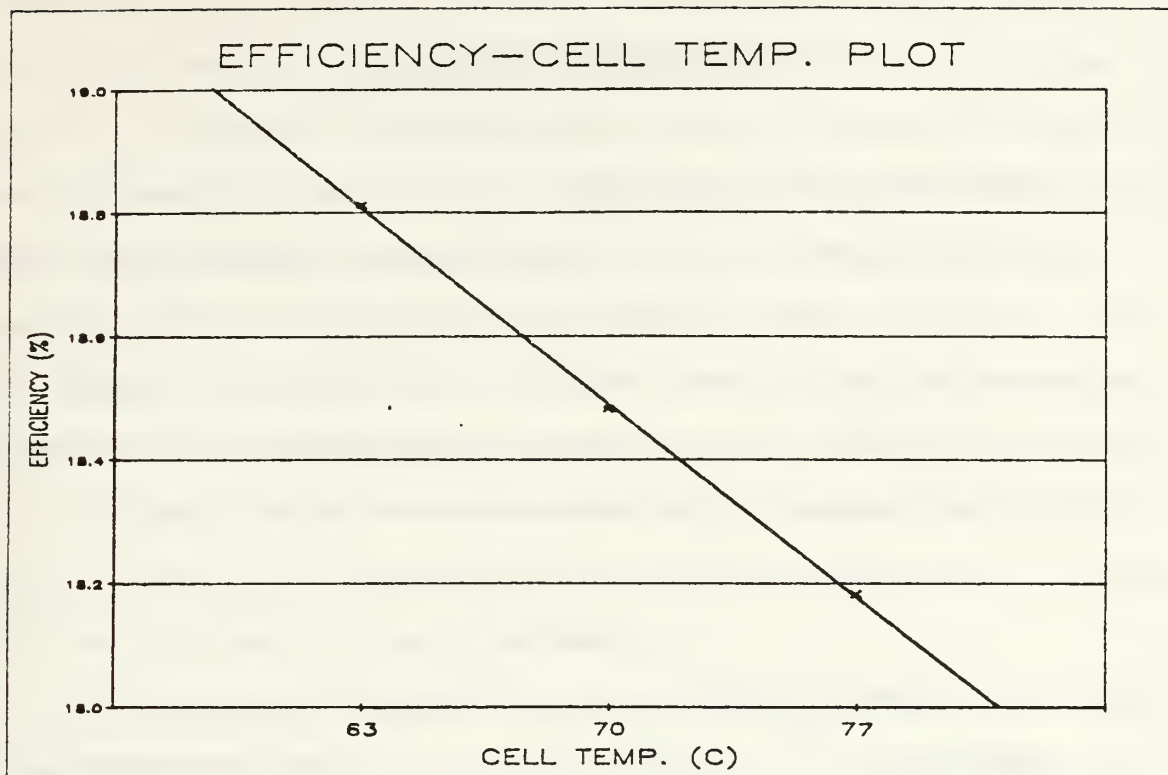


Figure 3 . The Cell Efficiency as a Function of Cell Temperature .

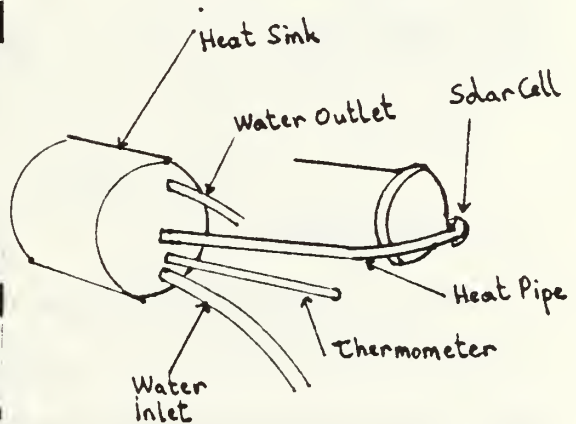
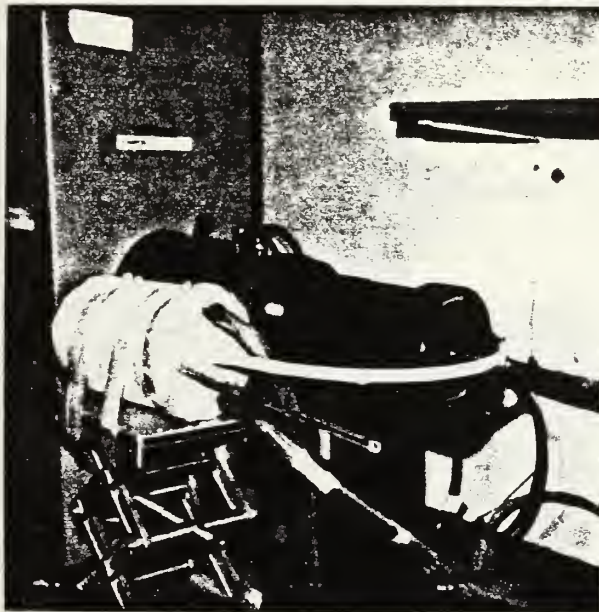


Figure 4. Photograph of the Heat Sink and Heat Pipe

IV. DISCUSSION OF TEST RESULTS

A. CONCENTRATOR ARRAY PERFORMANCE

In Table 4-1 the results which were measured until now, are compared to a flexible planar array. Planar array performance is found in Patterson [Ref. 5:p. 5]. From Table 4-1 it can be seen that using small unit concentrator systems in order to build an array, greater W/m^2 can be achieved. A picture of the unit concentrator is in Figure 5.

TABLE 4-1		
COMPARISON OF PLANAR AND CONCENTRATOR ARRAYS		
ARRAY TYPE	FLEXIBLE PLANAR	SMALL CONCENTRATOR
CELL T_{op}	68°C	77°C
P_{max} / A	147 W/m^2	246 W/m^2
P.F.	0.86	0.90
OPTIC EFF.	1	0.8
ARRAY POWER	126 W/m^2	177 W/m^2

B. ERROR ANALYSIS

Kratos spectral quality was discussed in Gold [Ref. 2:p. 38] and was found that there is an average of 1% difference between measurements made in NPS Laboratory and the ASEC values supplied with the solar cells. The close agreement was considered to be good. However, changes of Kratos supply voltage affects the light intensity of the Kratos lamp and

consequently the curve of the cell. In order to decrease the effect of sudden and short durational voltage changes, every data point in the I-V curve is measured 20 consecutive times. An average of these 20 measurements gives the data point itself. For perturbations which are not small and last for a long period of time, a necessity exists for repeating all tests from the starting point.

Resolution is 2.5 mV for the A/D converter and 2 mV for the power supply. All temperature measurements have an error of ± 0.5 K. Temperature measurements of the cell were recorded by a thermocouple, which is located very near to the cell on the test block. Thermal contact between the test block and the thermocouple is good.

The computation of cell performance is based on a Space Environment temperature of $T_s = 0$ K; but this is not the case always. The value of T_s can change depending on the position of the space vehicle and time.

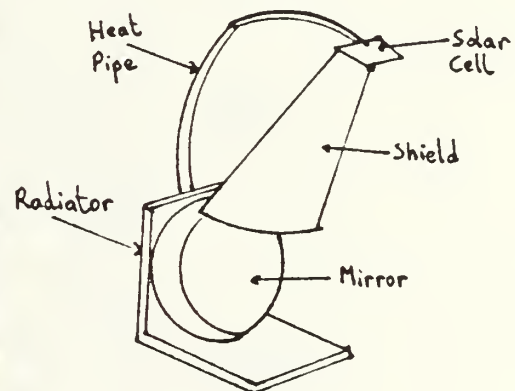


Figure 5. Photograph of the Unit Concentrator

V. RECOMMENDATIONS

One advantage of a concentrator system is shielding against radiation of charged particles and space dusts (micrometeoroid erosion). The GaAs solar cells tested in this thesis should be irradiated with high energy electrons. The cells should be located within the solar concentrator to validate the level of shielding which is anticipated.

In this thesis, because of the low reflectivity of the mirror(0.8), light was reflected only one time. If durable mirrors with higher reflectivity are available, a Cassegrain type small concentrator is more attractive because of economy and the ease of the design. Reference to Figure 6 shows that for a Cassegrain optical arrangement a heat pipe will not be necessary. Further, it can be assumed that, a Cassegrain system will give more radiation protection because of the geometry.

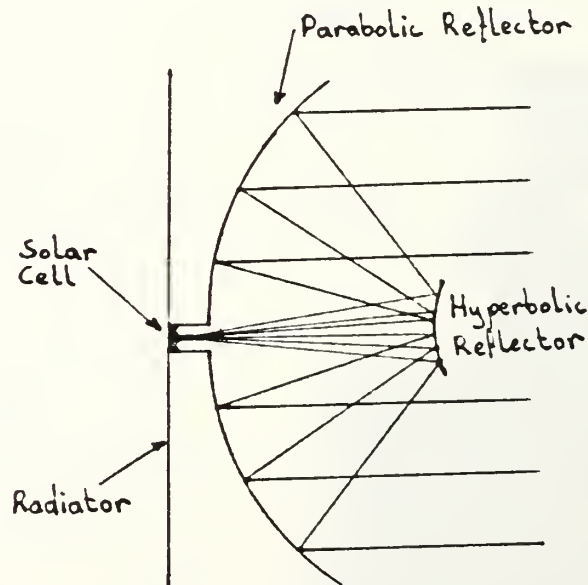


Figure 6. Cassegrain Type Modular Concentrator

APPENDIX A

CELL CURRENT-VOLTAGE CURVES

Table 3-1 reports the efficiency for the various cells at $C = 1$. Figure 7 to 12 report current-voltage (I-V) curves for cells 1 to 6 for $T = 28^{\circ}\text{C}$. The information provided by the curves includes I_{sc} , V_{oc} , P_{max} , V_{max} , I_{max} , FF and efficiency. Similar data are shown in Figure 13 to 18 for same conditions except $C \cong 130$. Figures 19 to 24 show I-V curves for $T = 77^{\circ}\text{C}$ and $C \cong 130$. The same data from Figures 7 to 12 and from Figure 13 to 18 are replotted using a semi-log scale for comparison purposes. A very large change in current occurs. The change in voltage (V_{oc}) is minor.

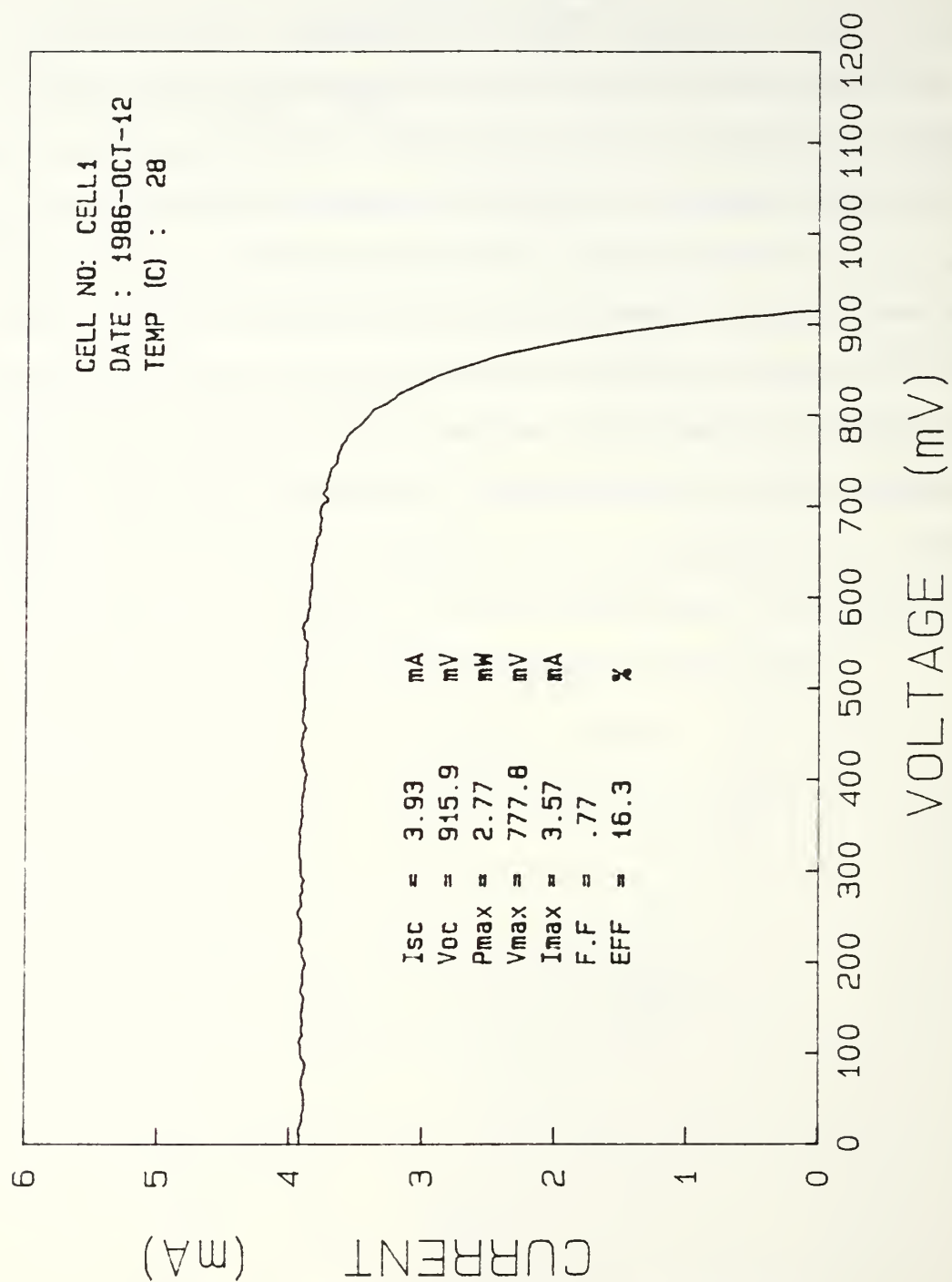


Figure 7. I-V Curve from CELL1

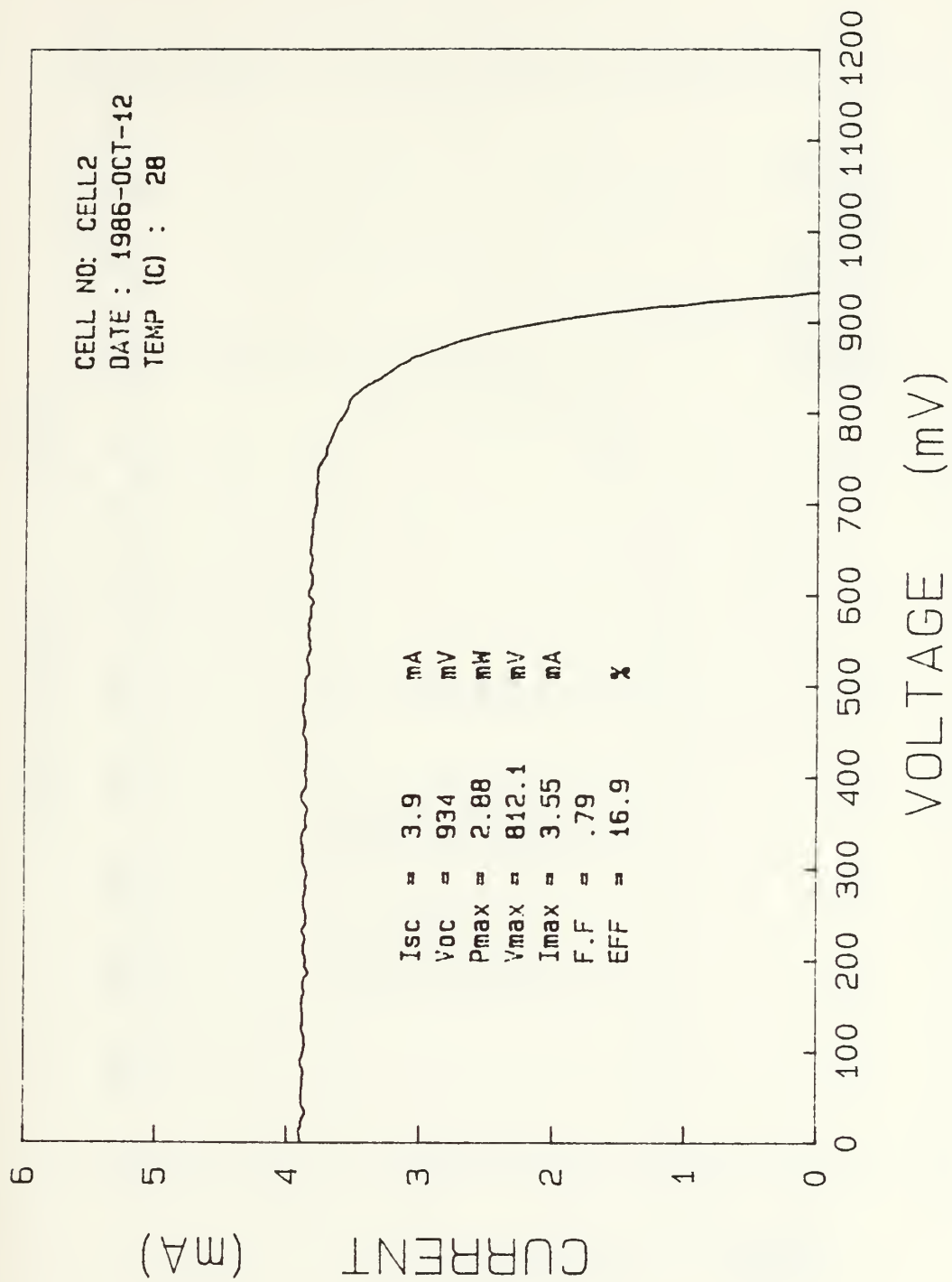


Figure 8. I-V Curve from CELL2

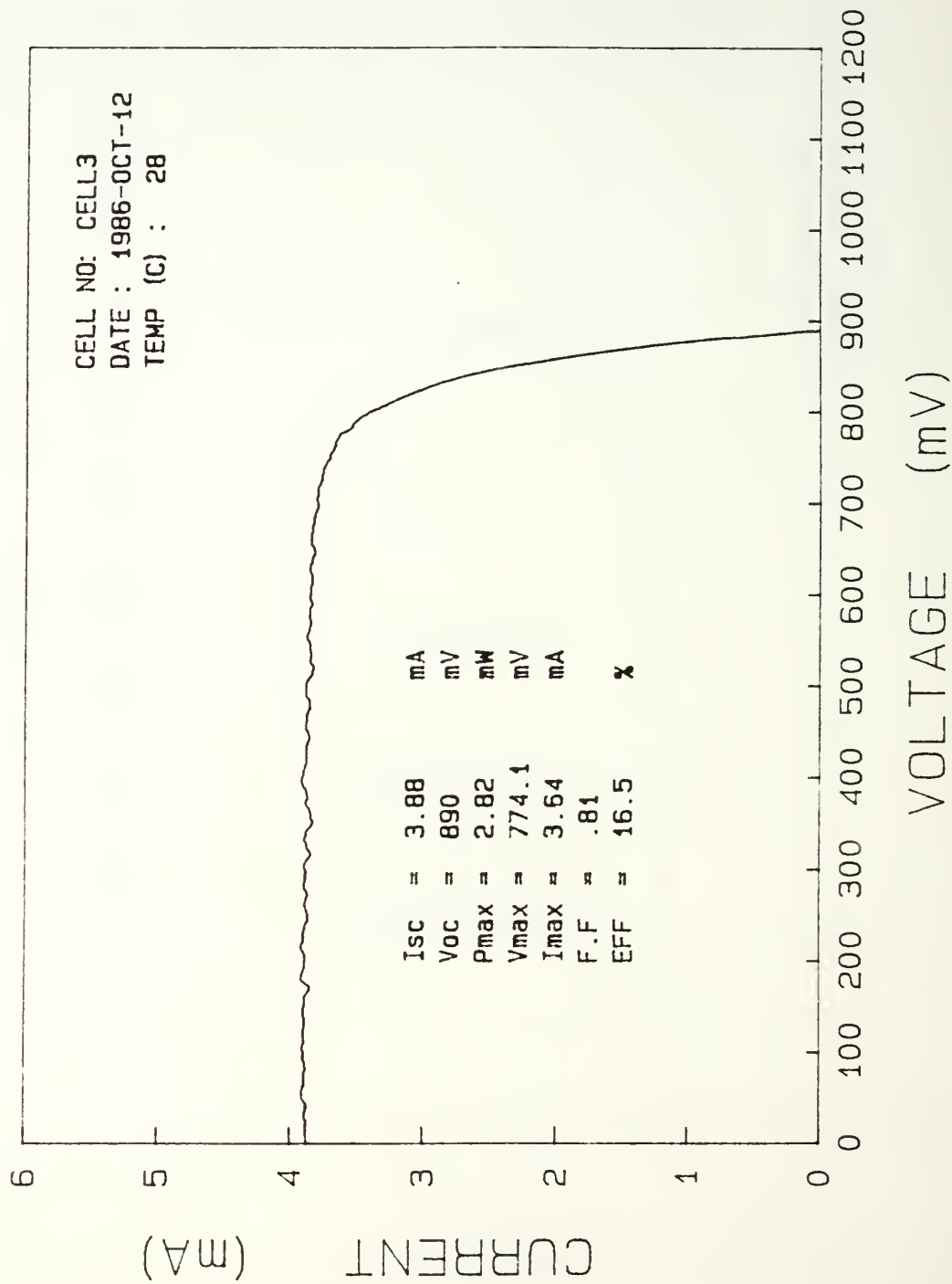


Figure 9. I-V Curve from CELL3

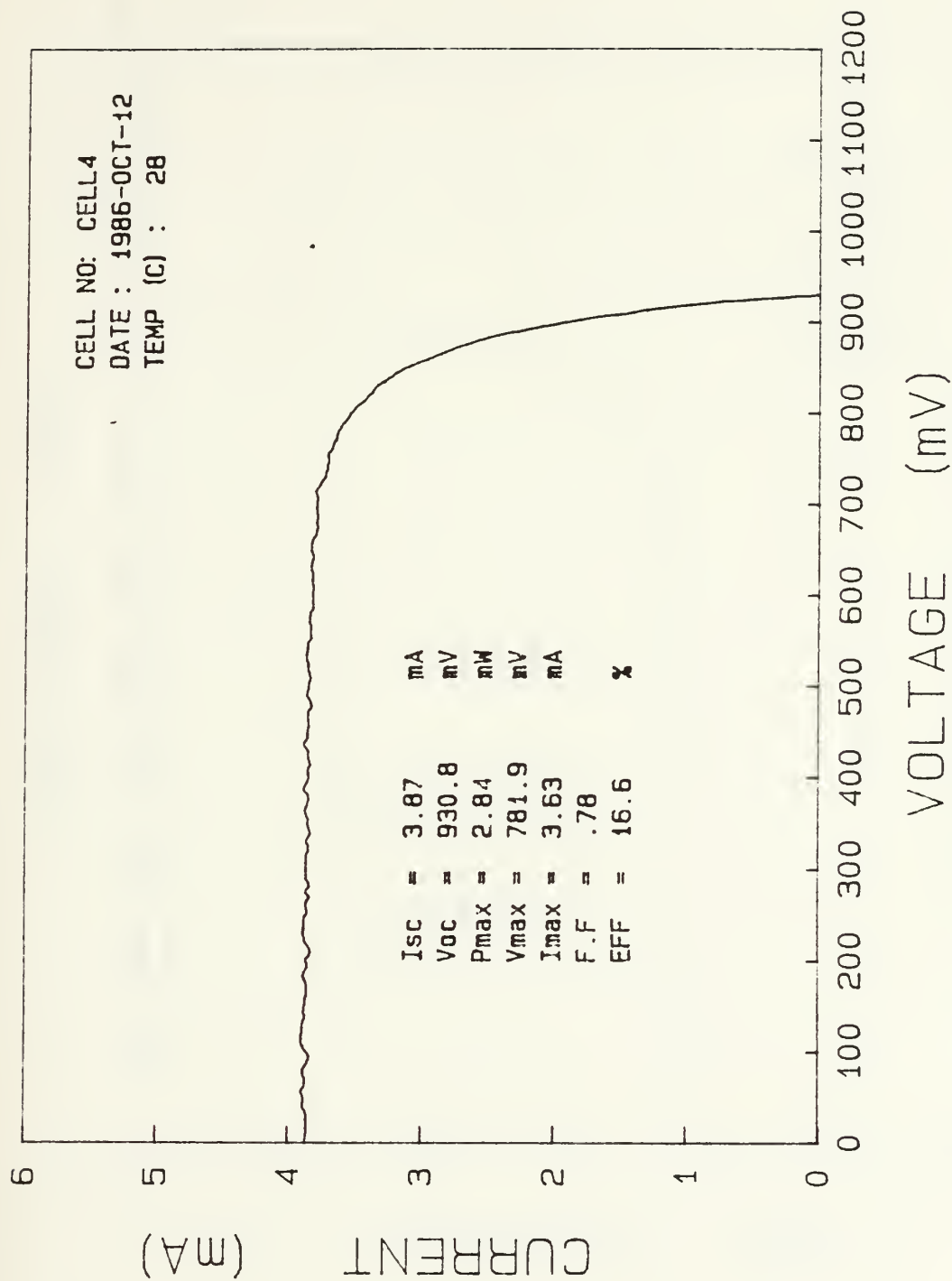


Figure 10. I-V Curve from CELL4

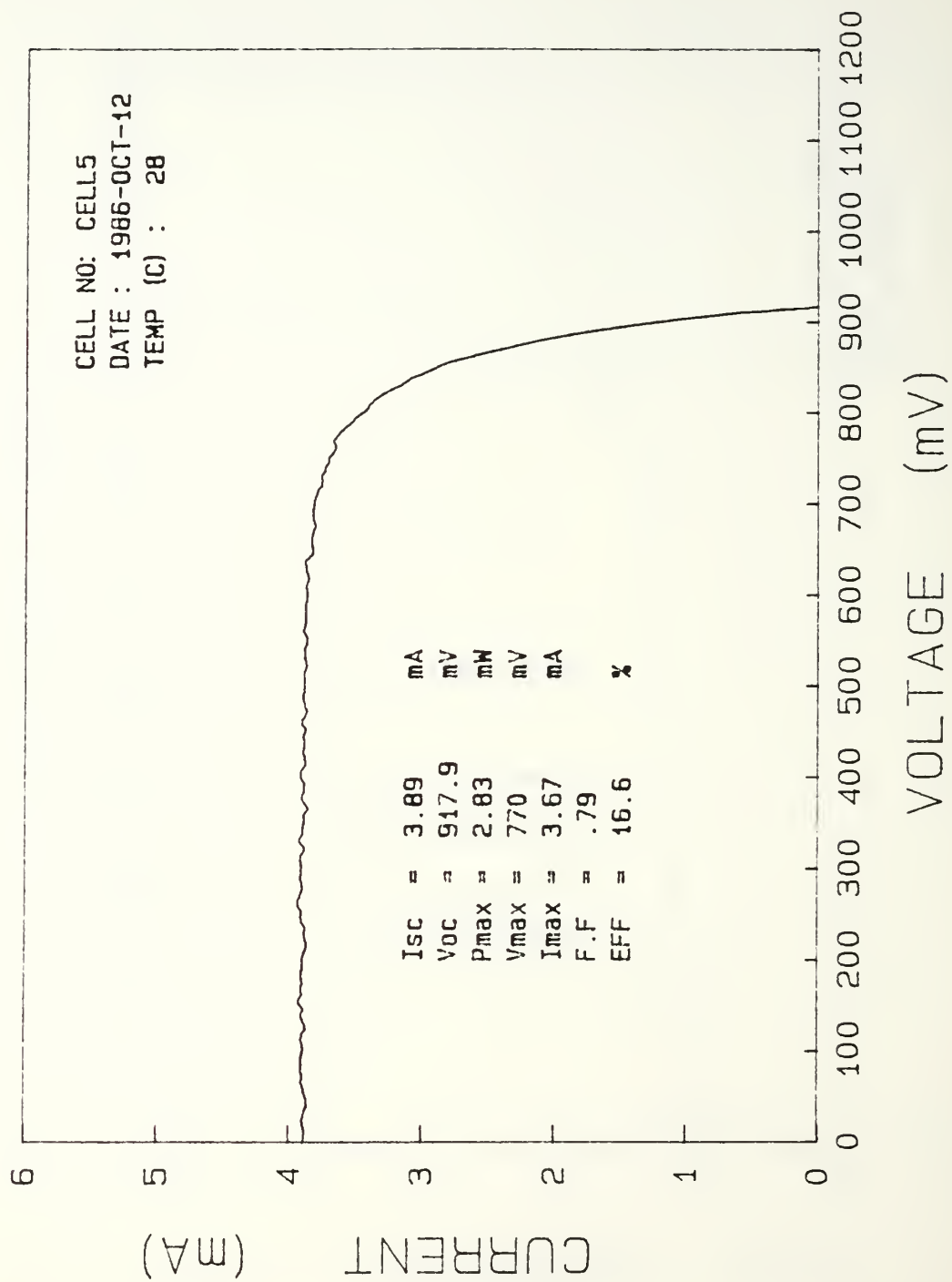


Figure 11. I-V Curve from CELL5

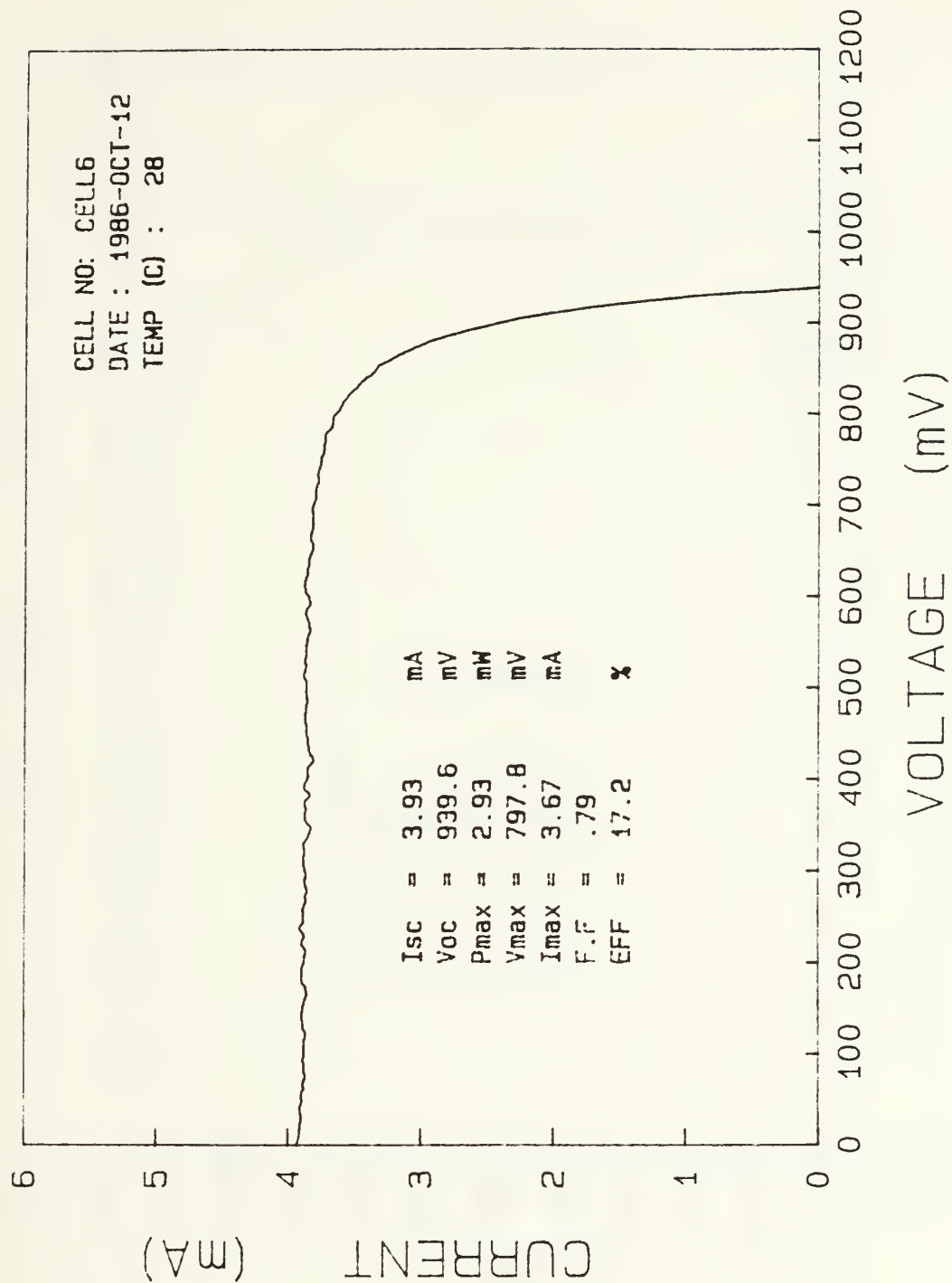


Figure 12. I-V Curve from CELL6

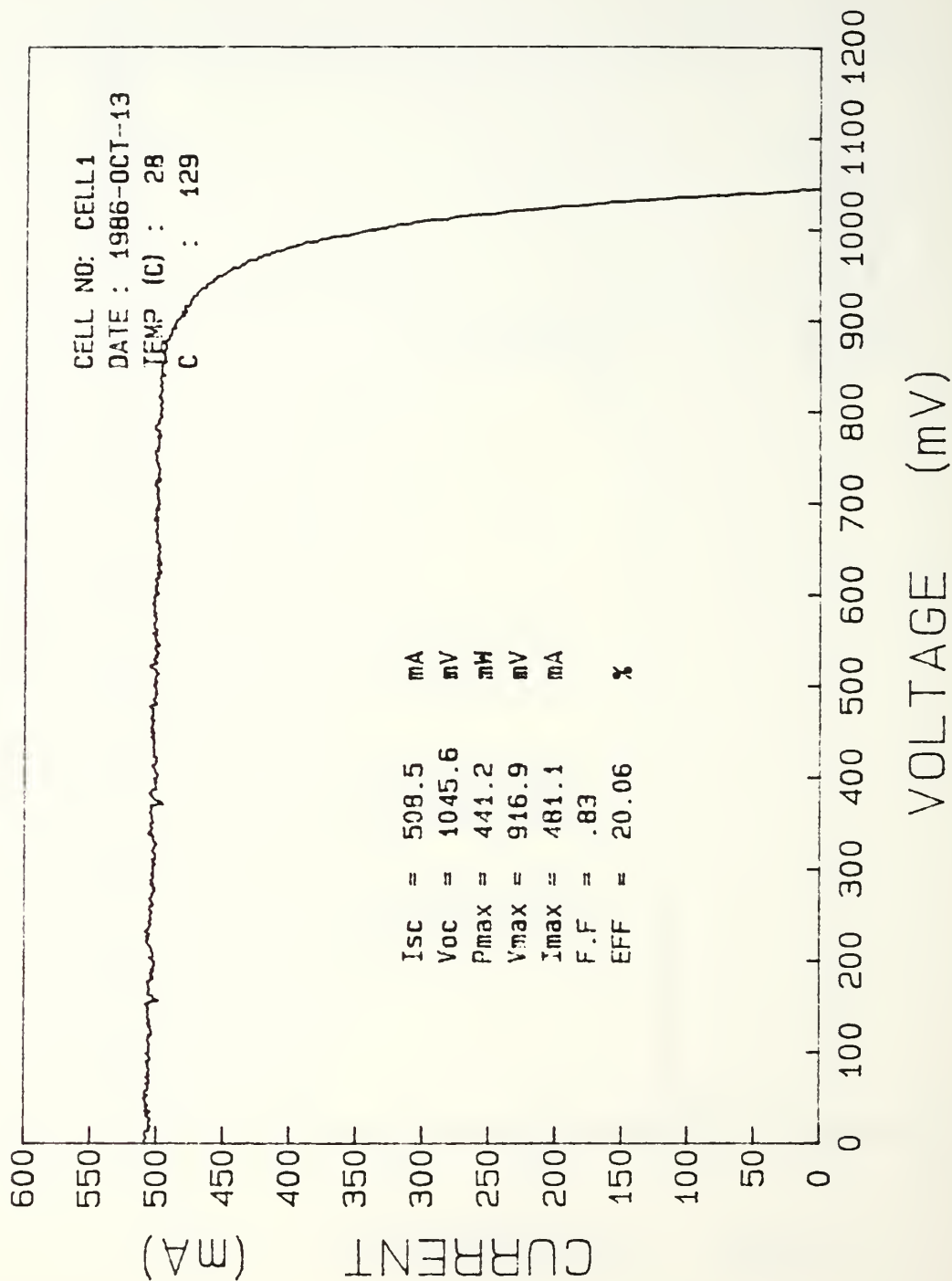


Figure 13. I-V Curve from CELL1

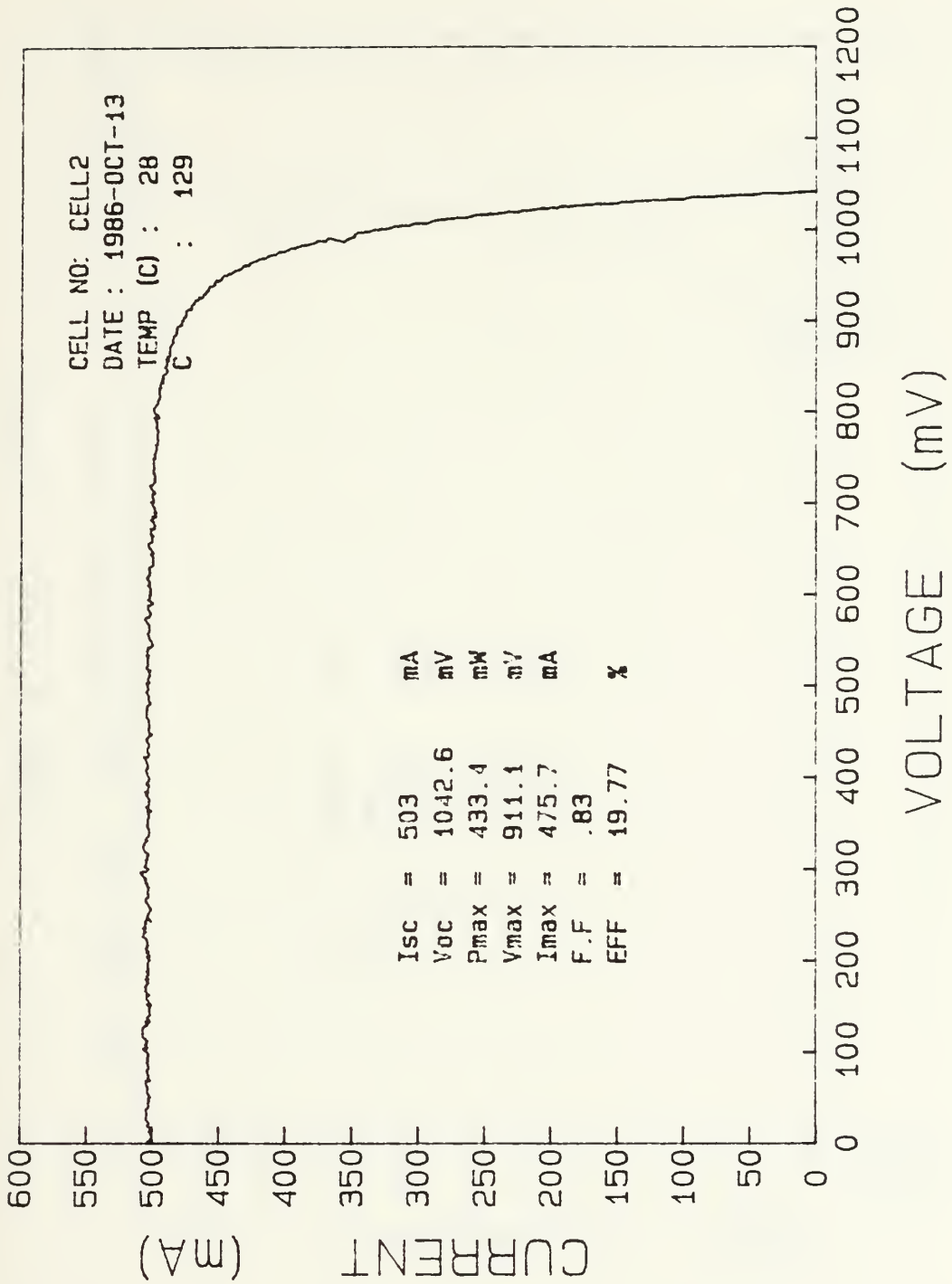


Figure 14. I-V Curve from CELL2

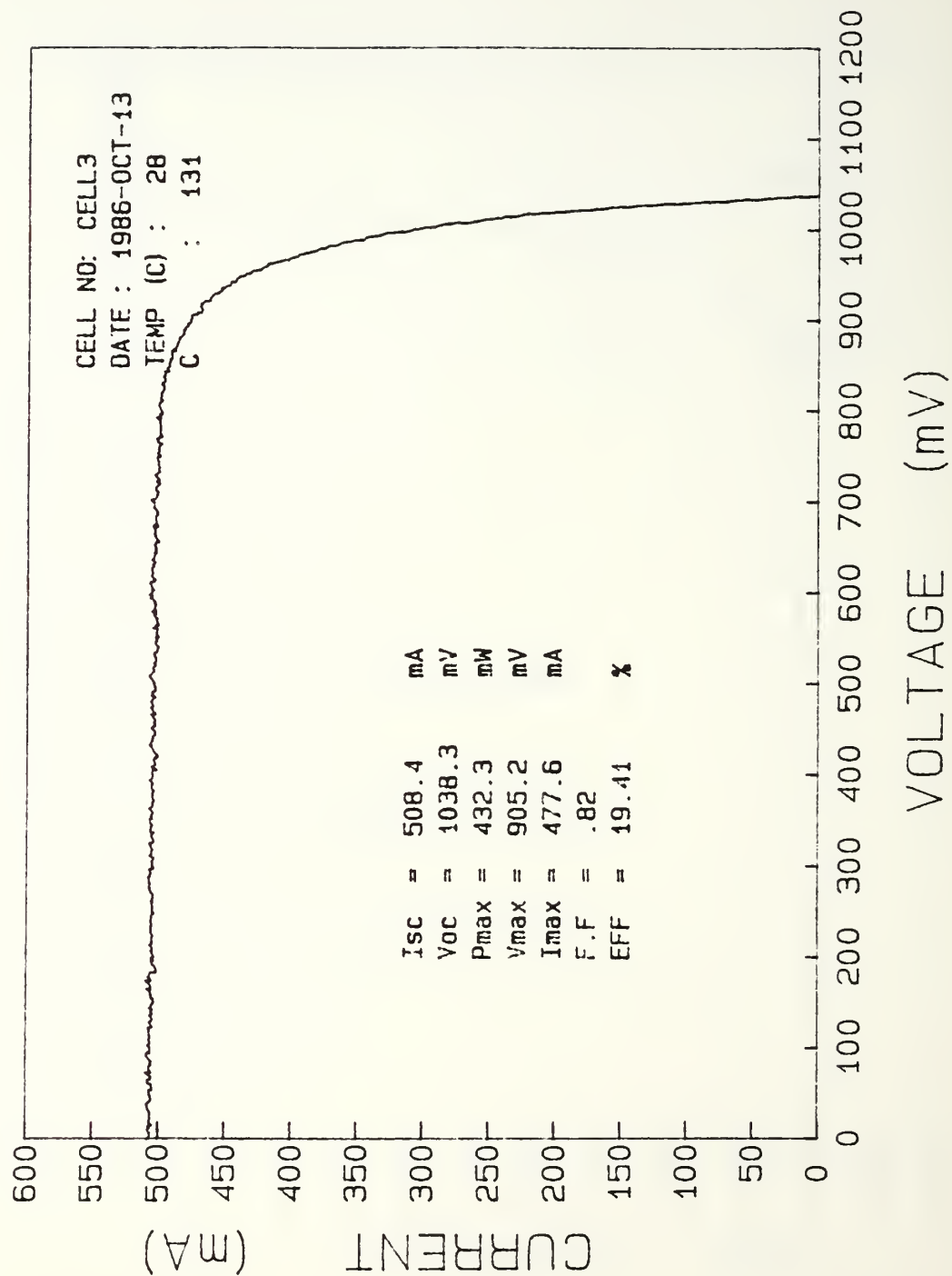


Figure 15. I-V Curve from CELL3

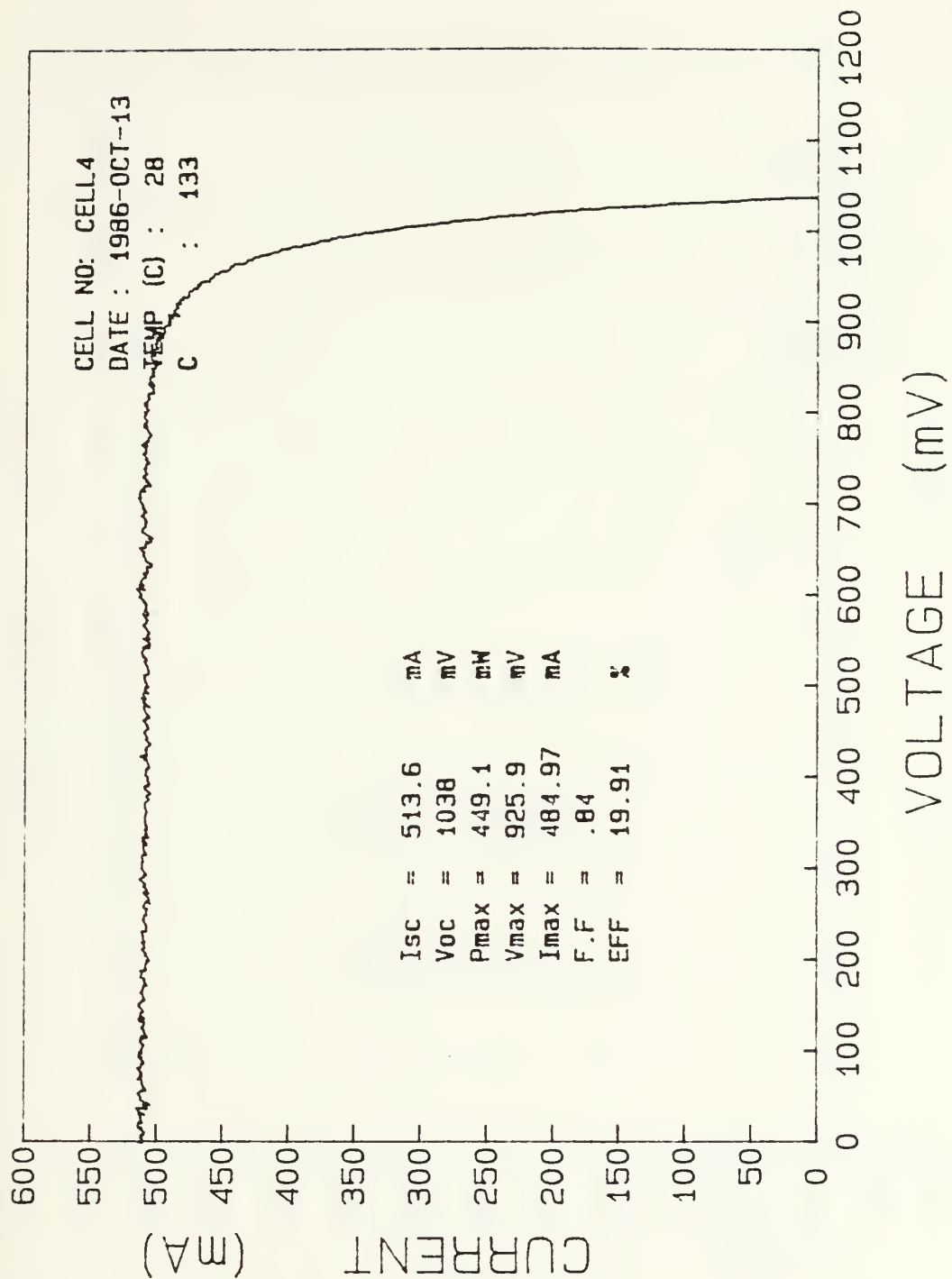


Figure 16. I-V Curve from CELL4

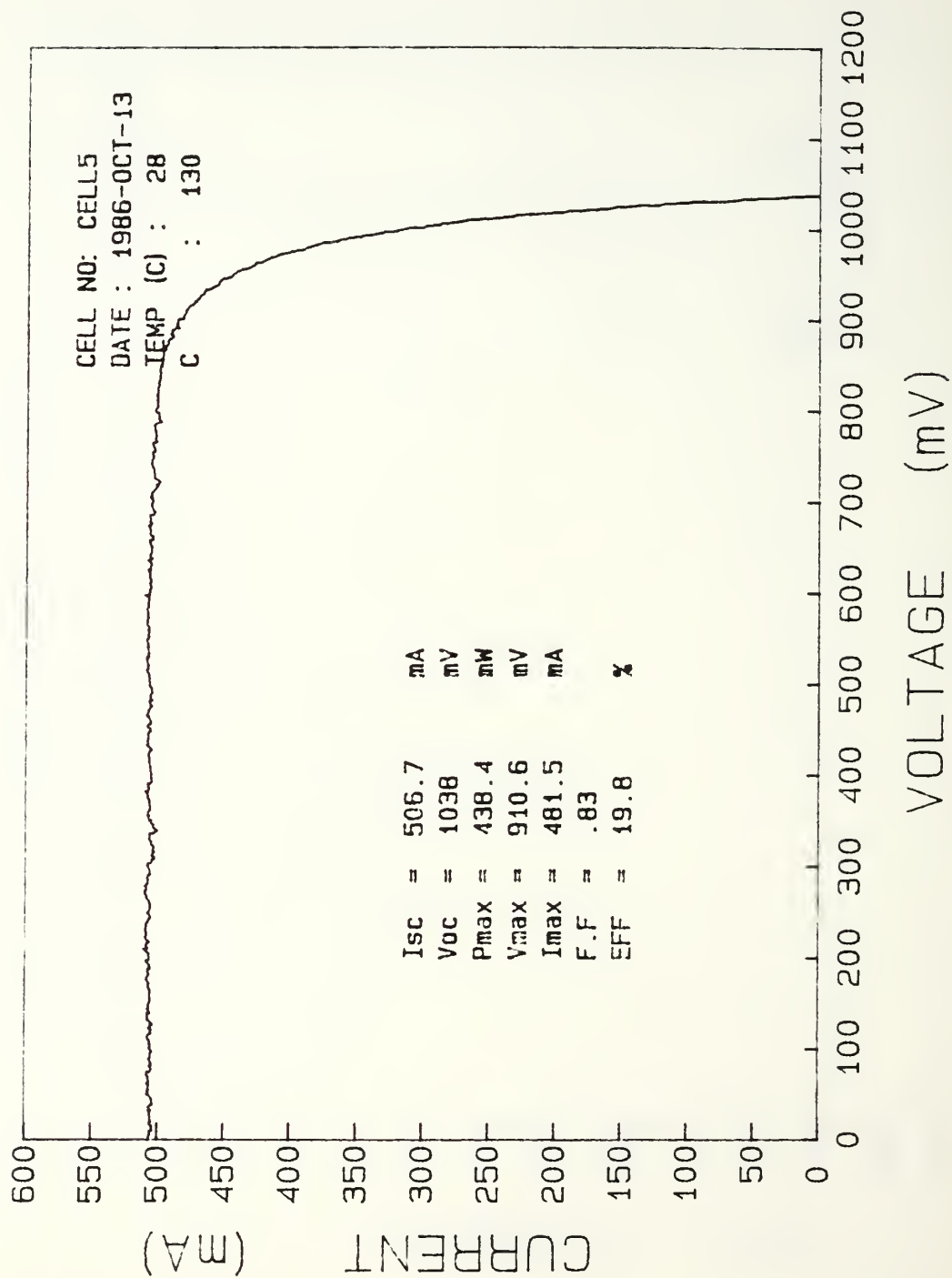


Figure 17. I-V Curve from CELL5

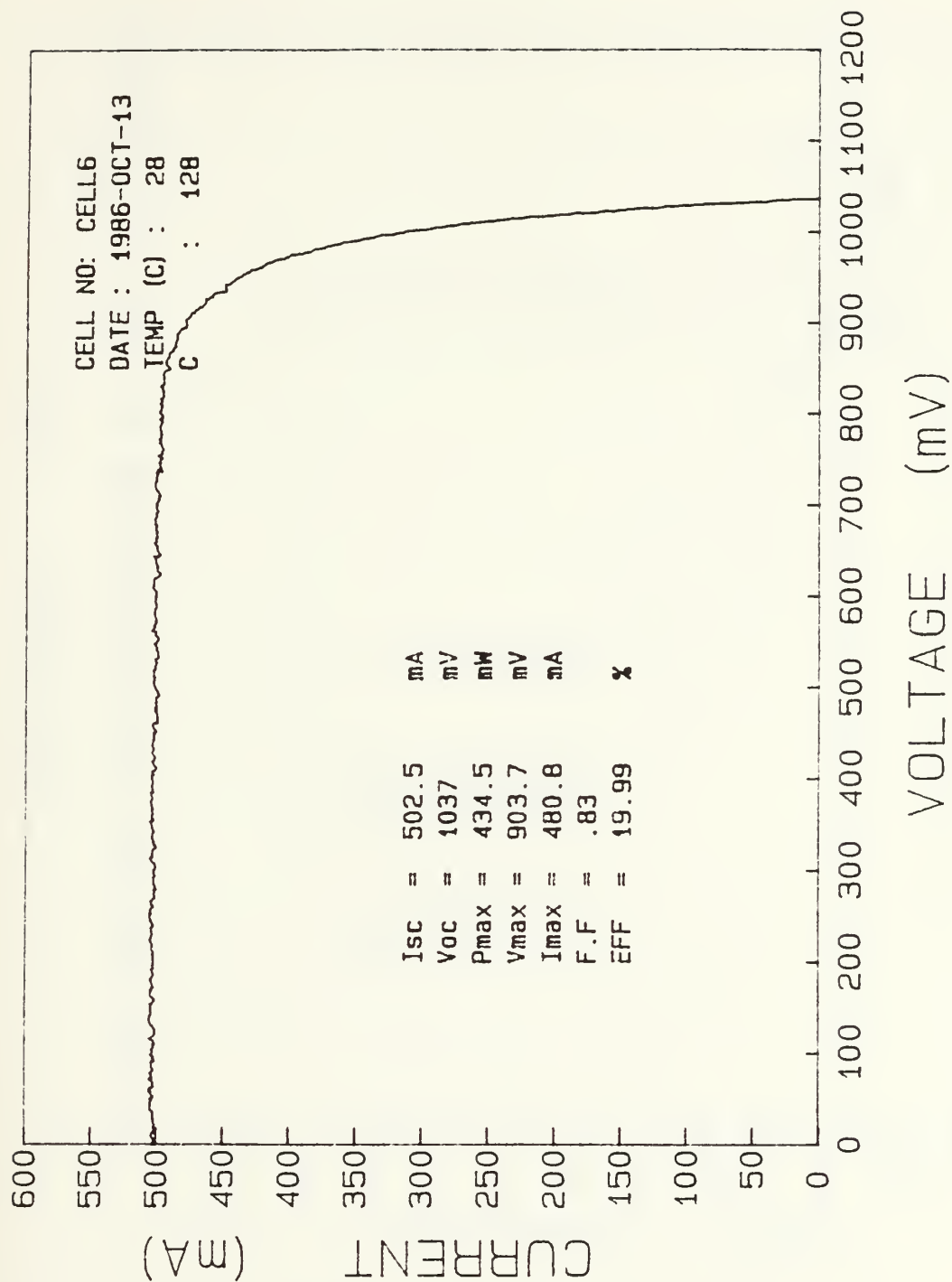


Figure 18. I-V Curve from CELL6

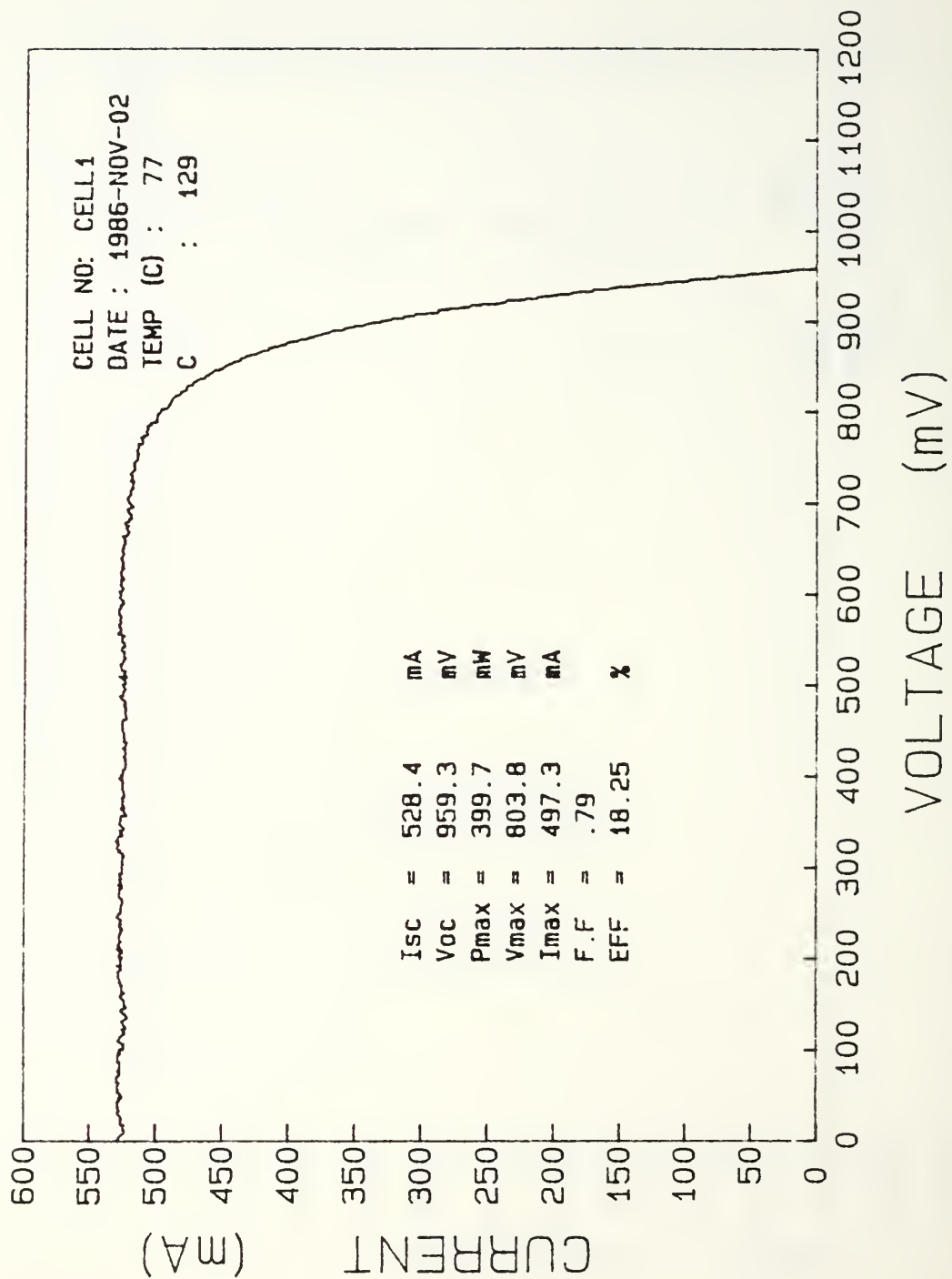


Figure 19. I-V Curve from CELL1

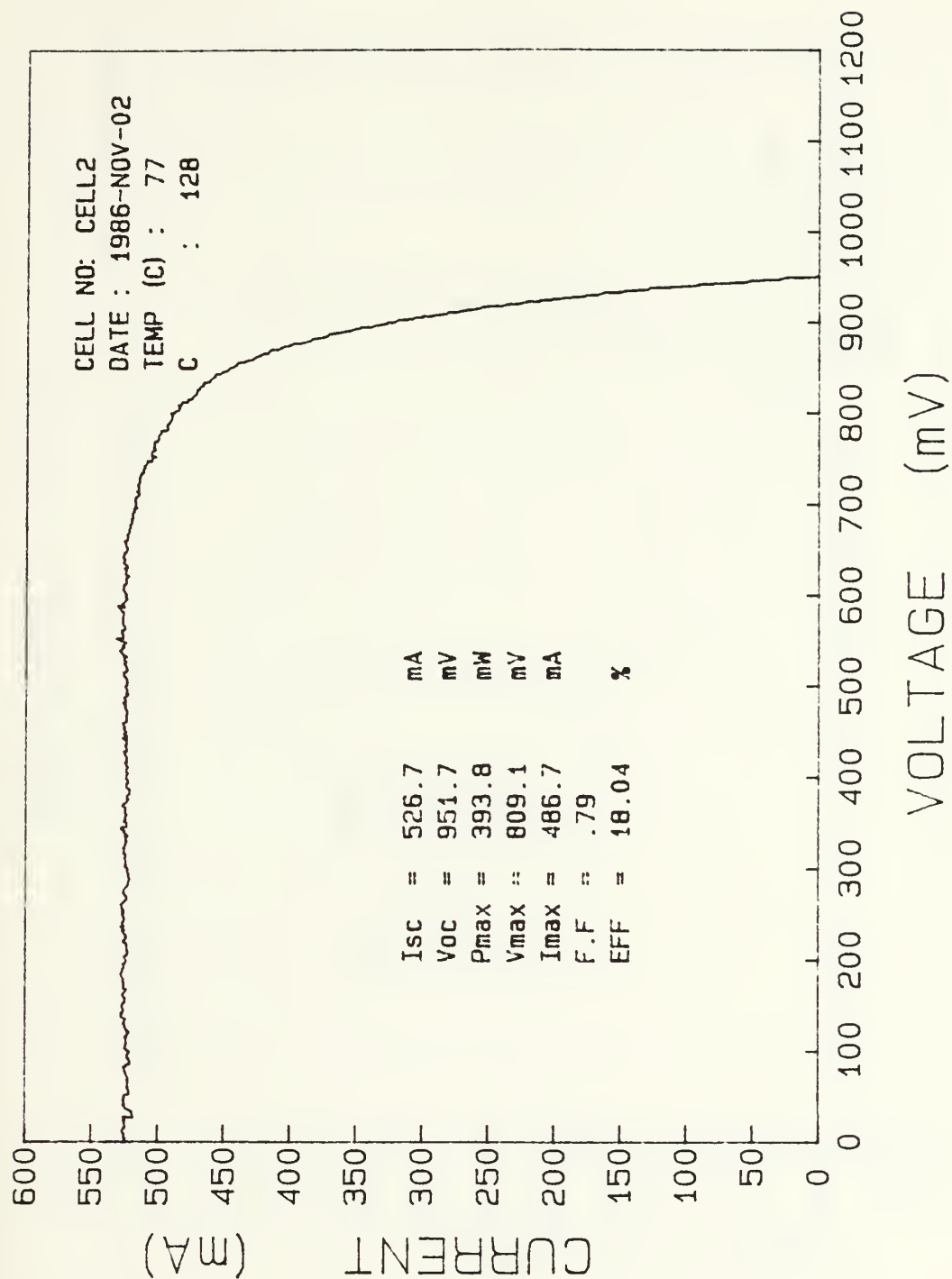


Figure 20. I-V Curve from CELL2

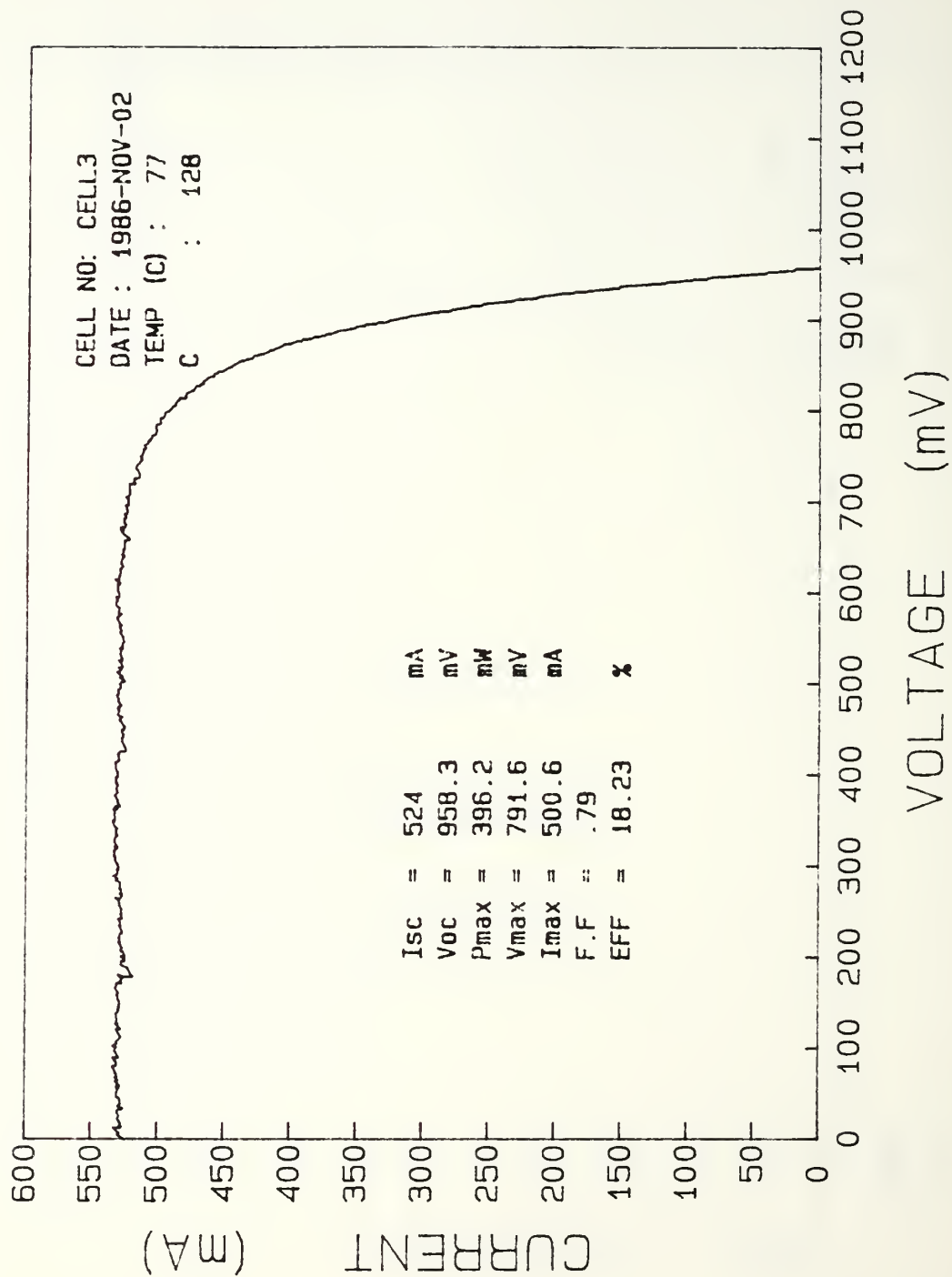


Figure 21. I-V Curve from CELL3

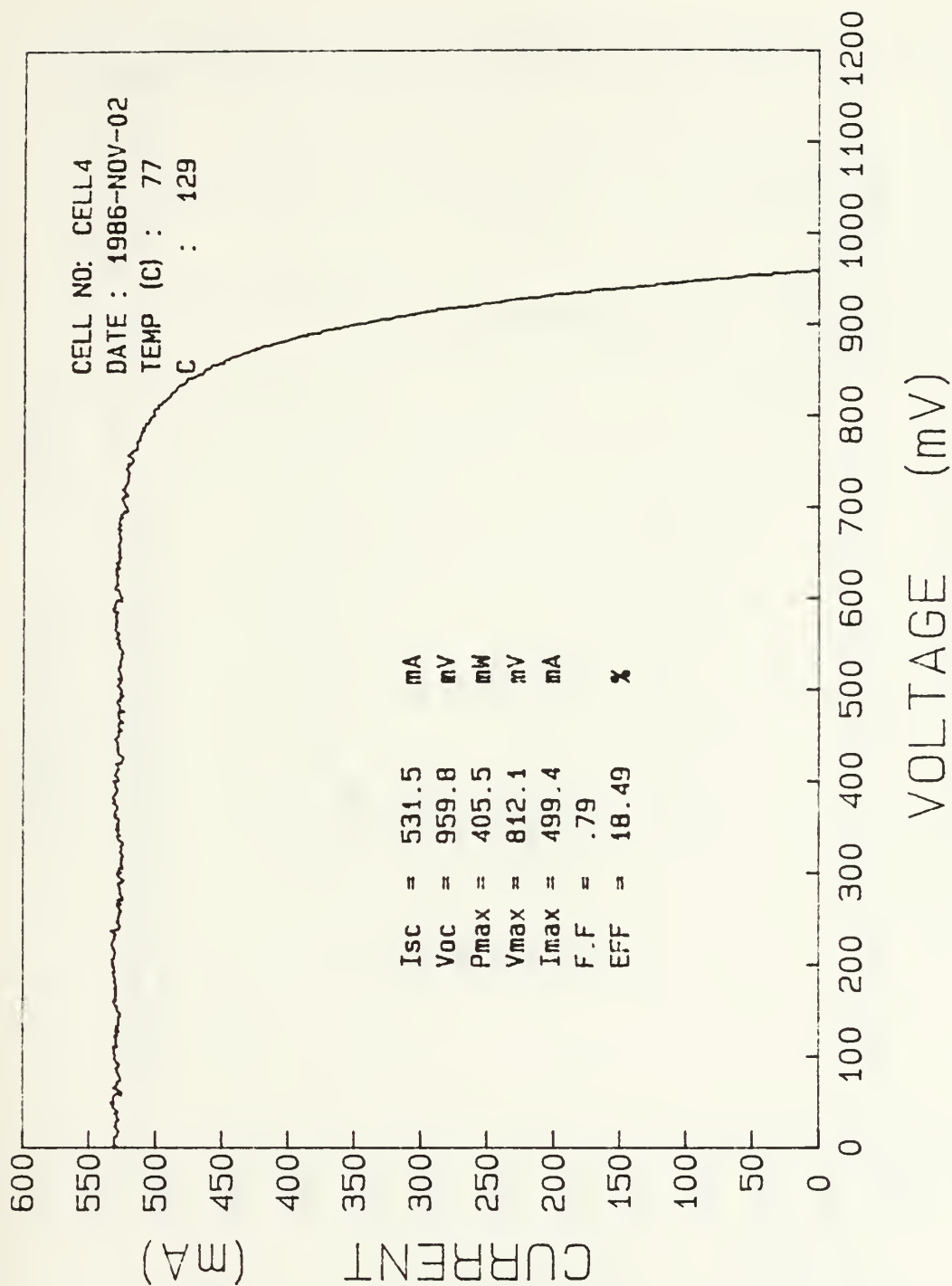


Figure 22. I-V Curve from CELL4

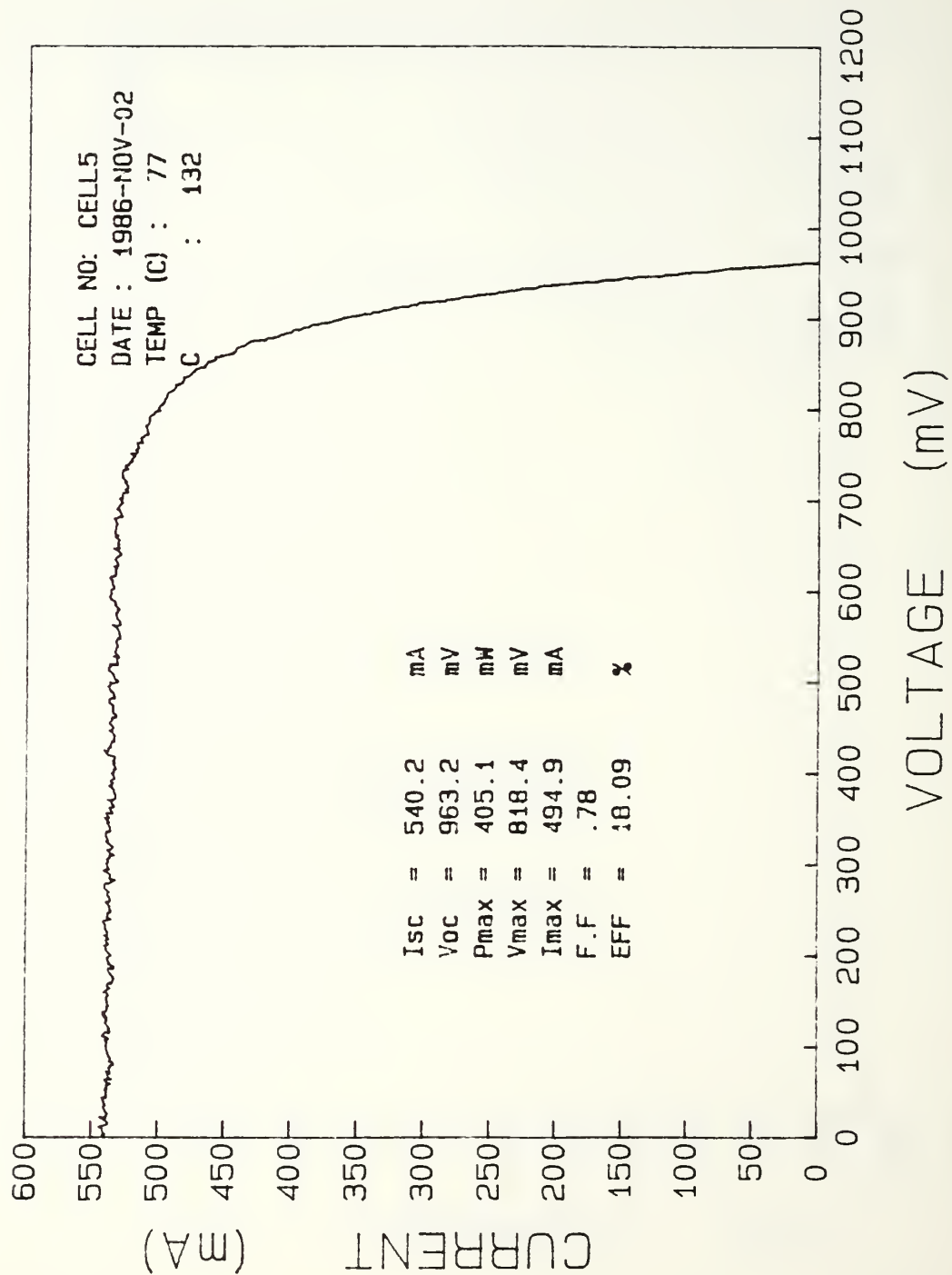


Figure 23. I-V Curve from CELL5

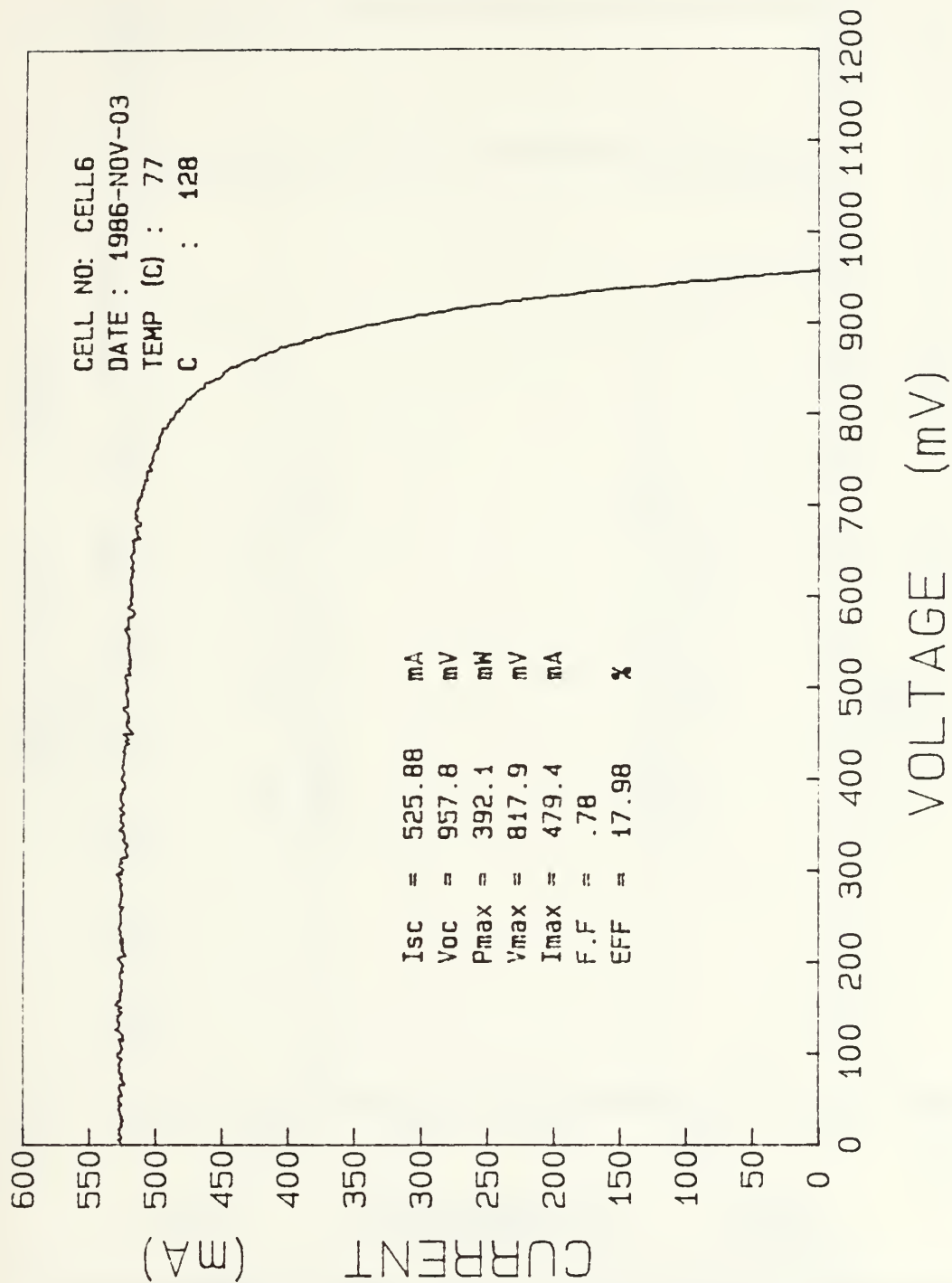


Figure 24. I-V Curve from CELL6

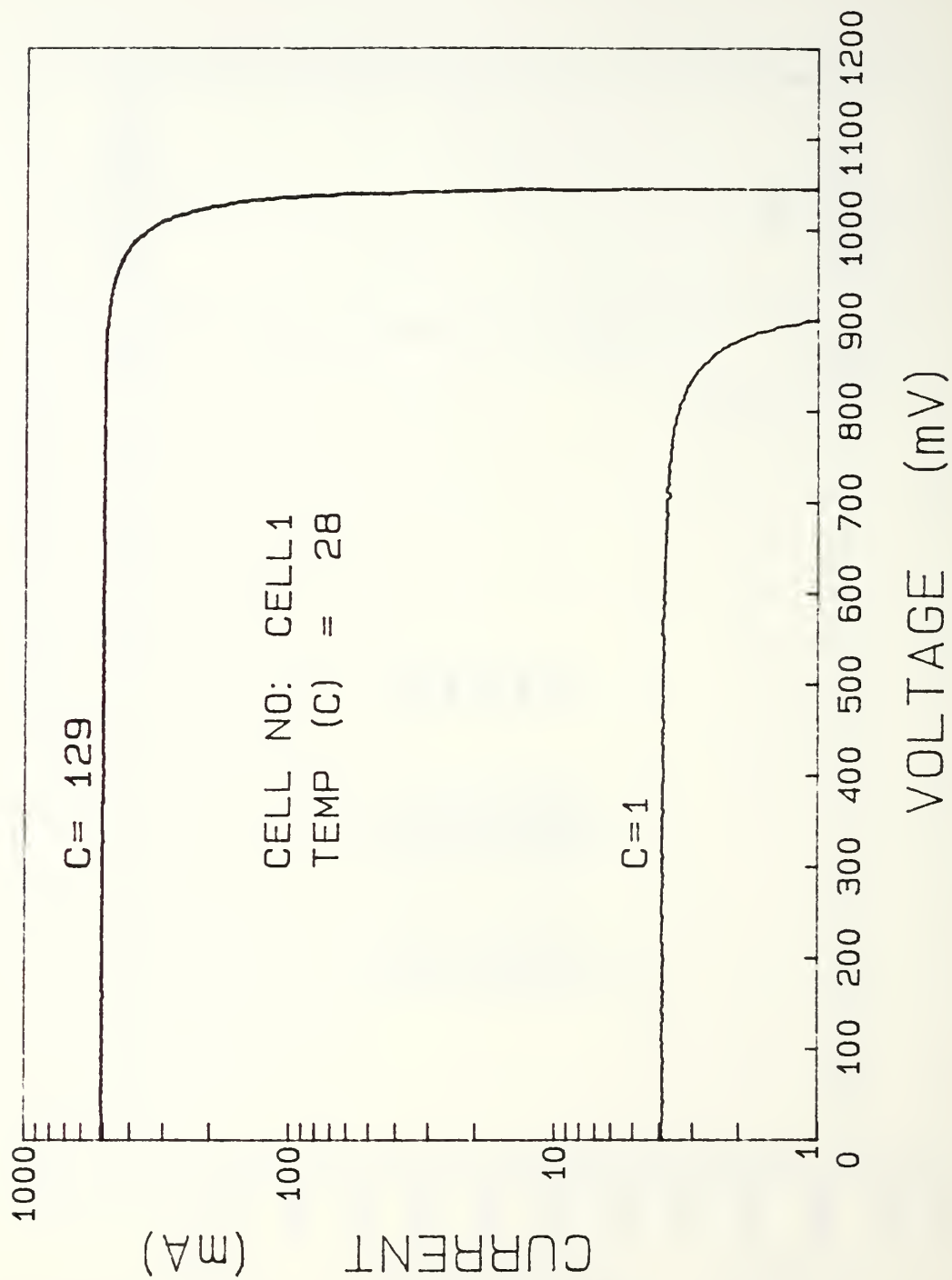


Figure 25. Comparison of Cell I-V Curves with Different Concentration Levels

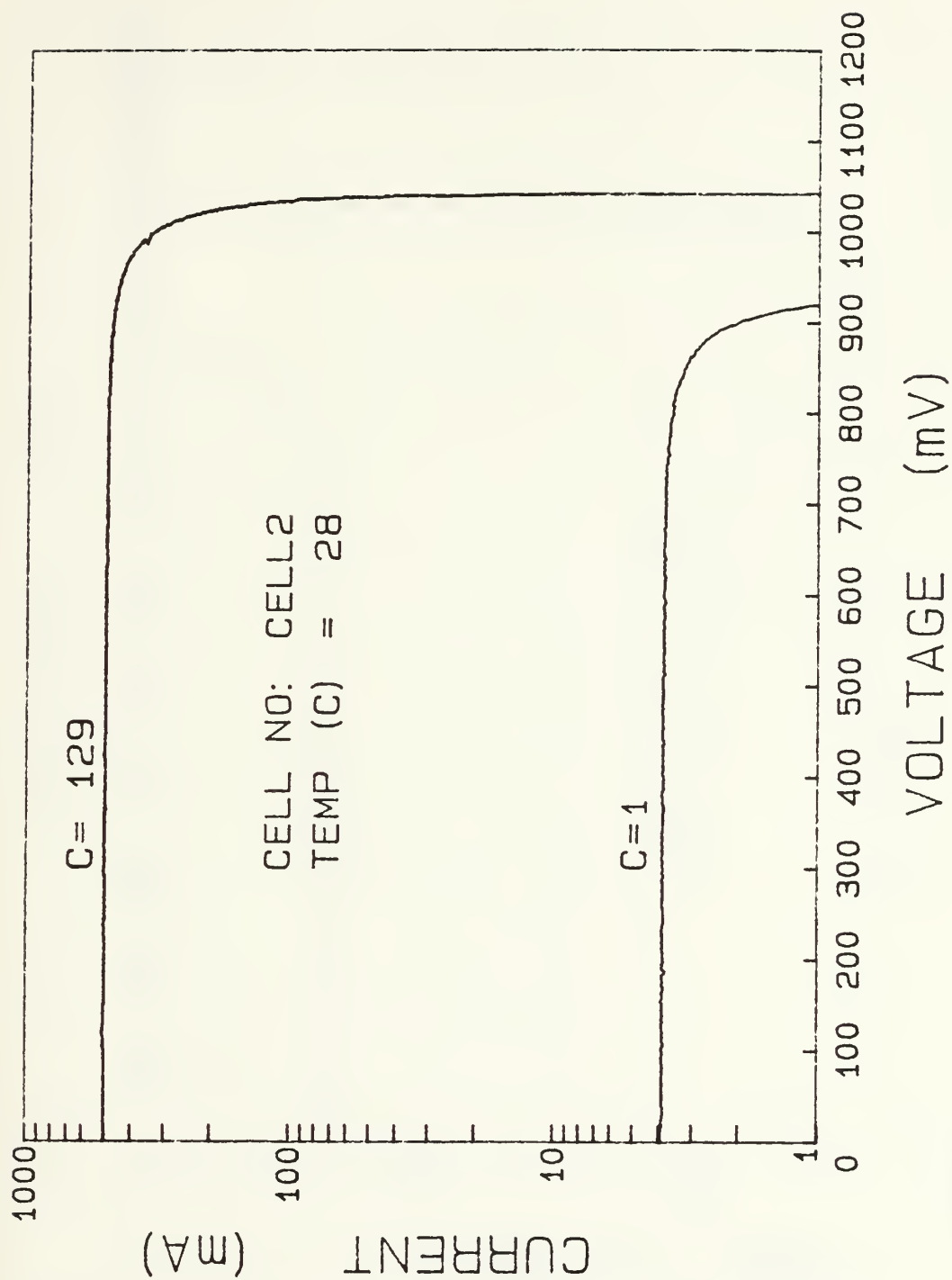


Figure 26. Comparison of Cell I-V Curves with Different Concentration Levels

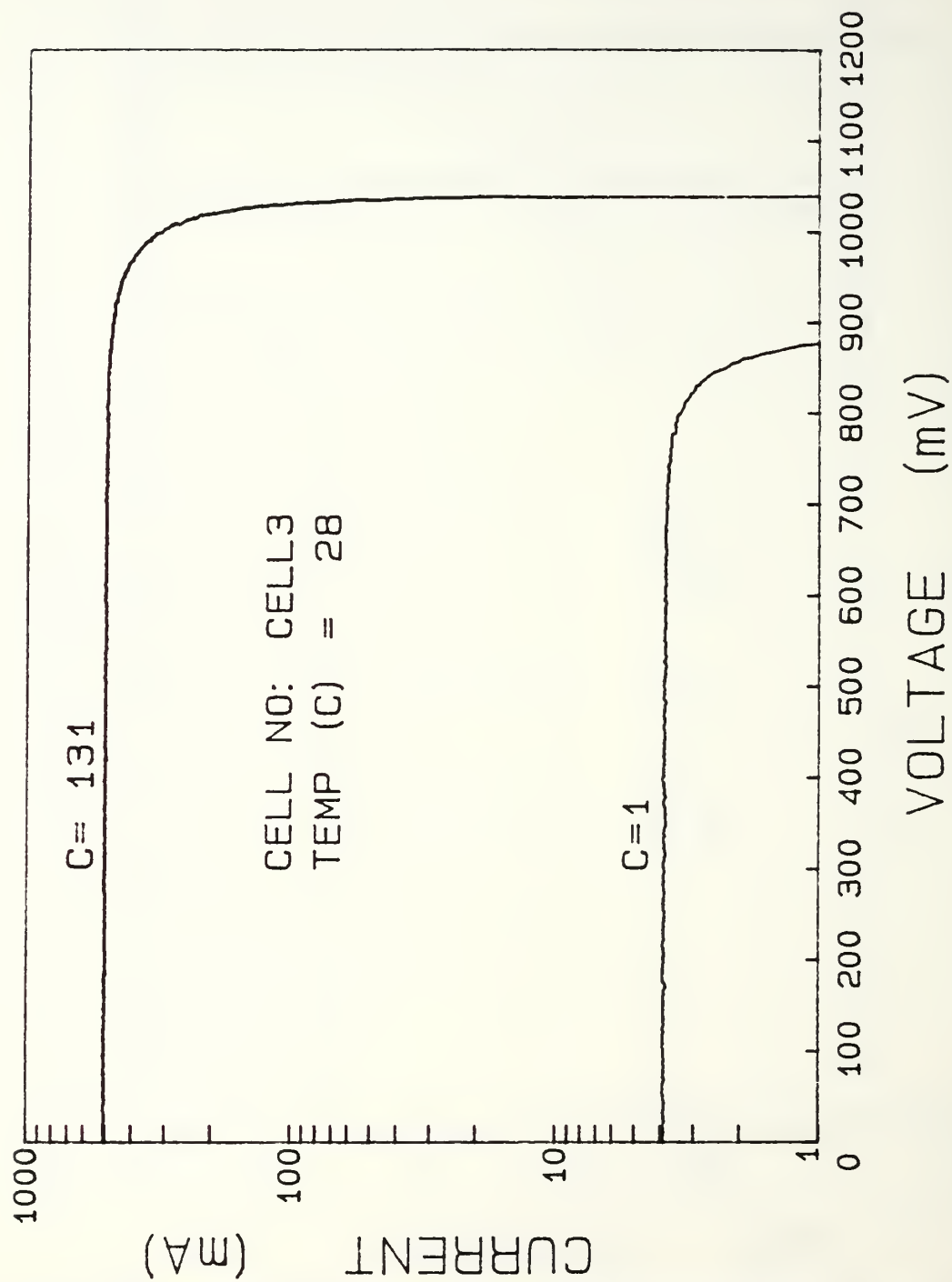


Figure 27. Comparison of Cell I-V Curves with Different Concentration Levels

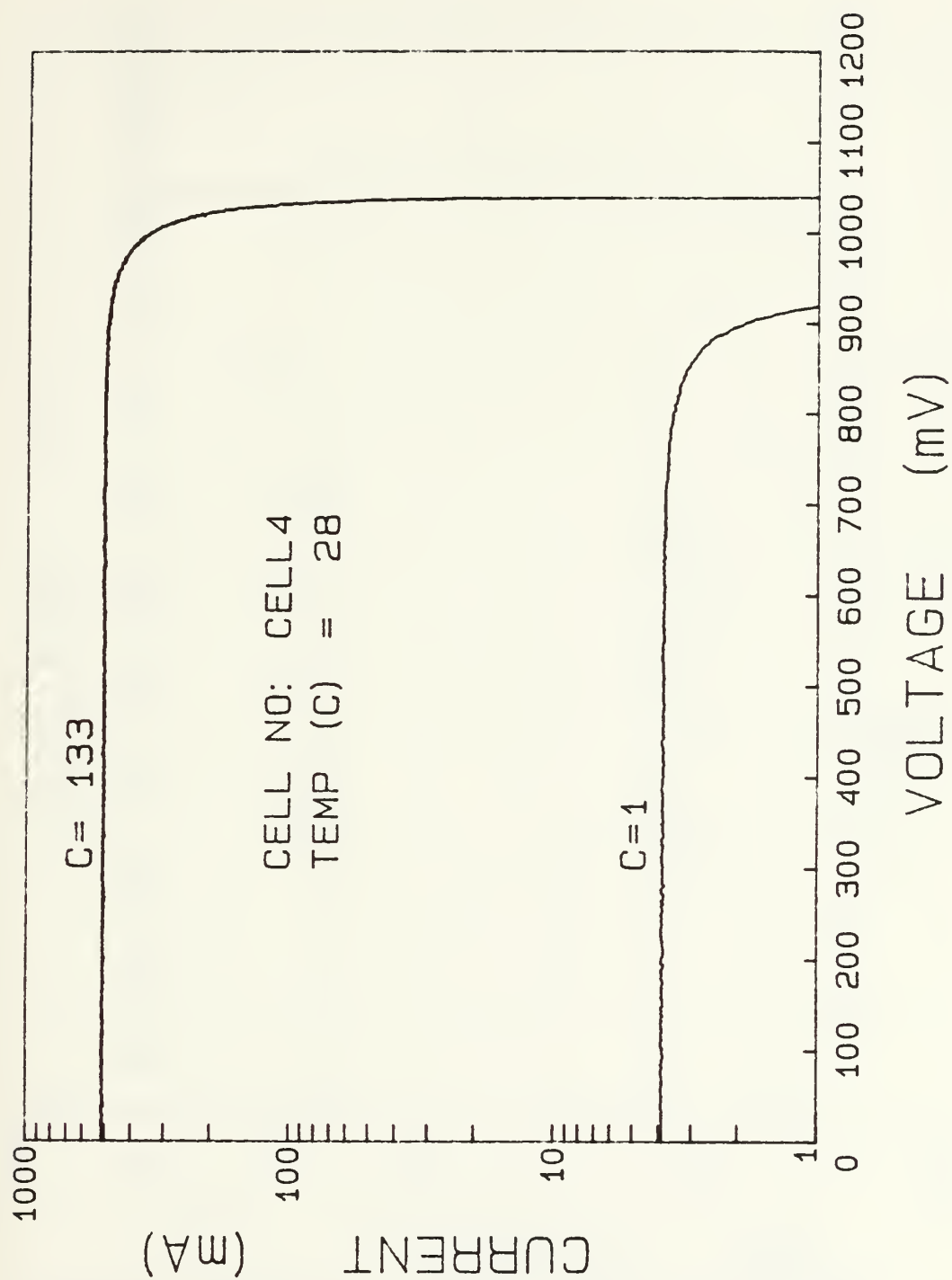


Figure 28. Comparison of Cell I-V Curves with Different Concentration Levels

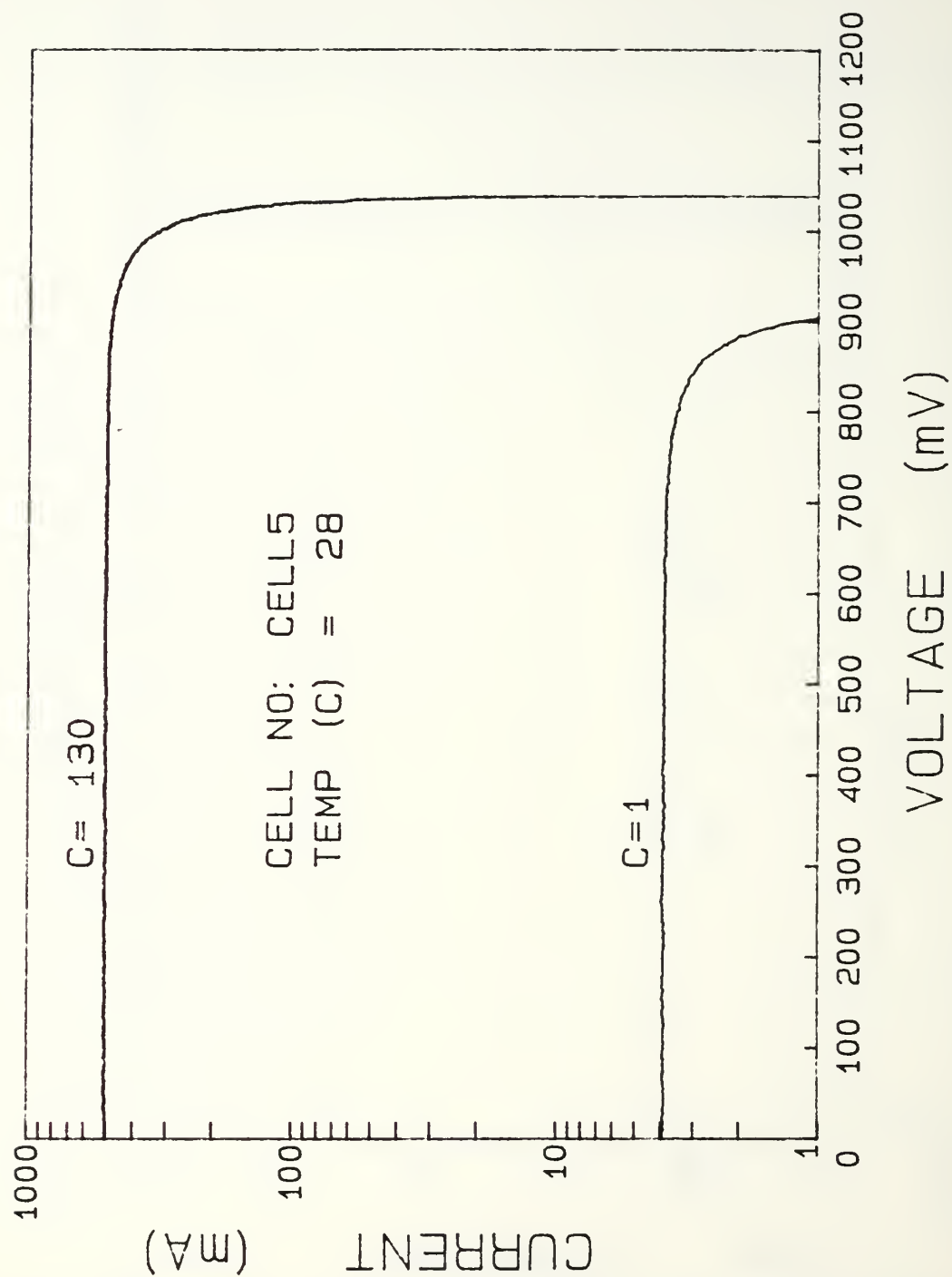


Figure 29. Comparison of Cell I-V Curves with Different Concentration Levels

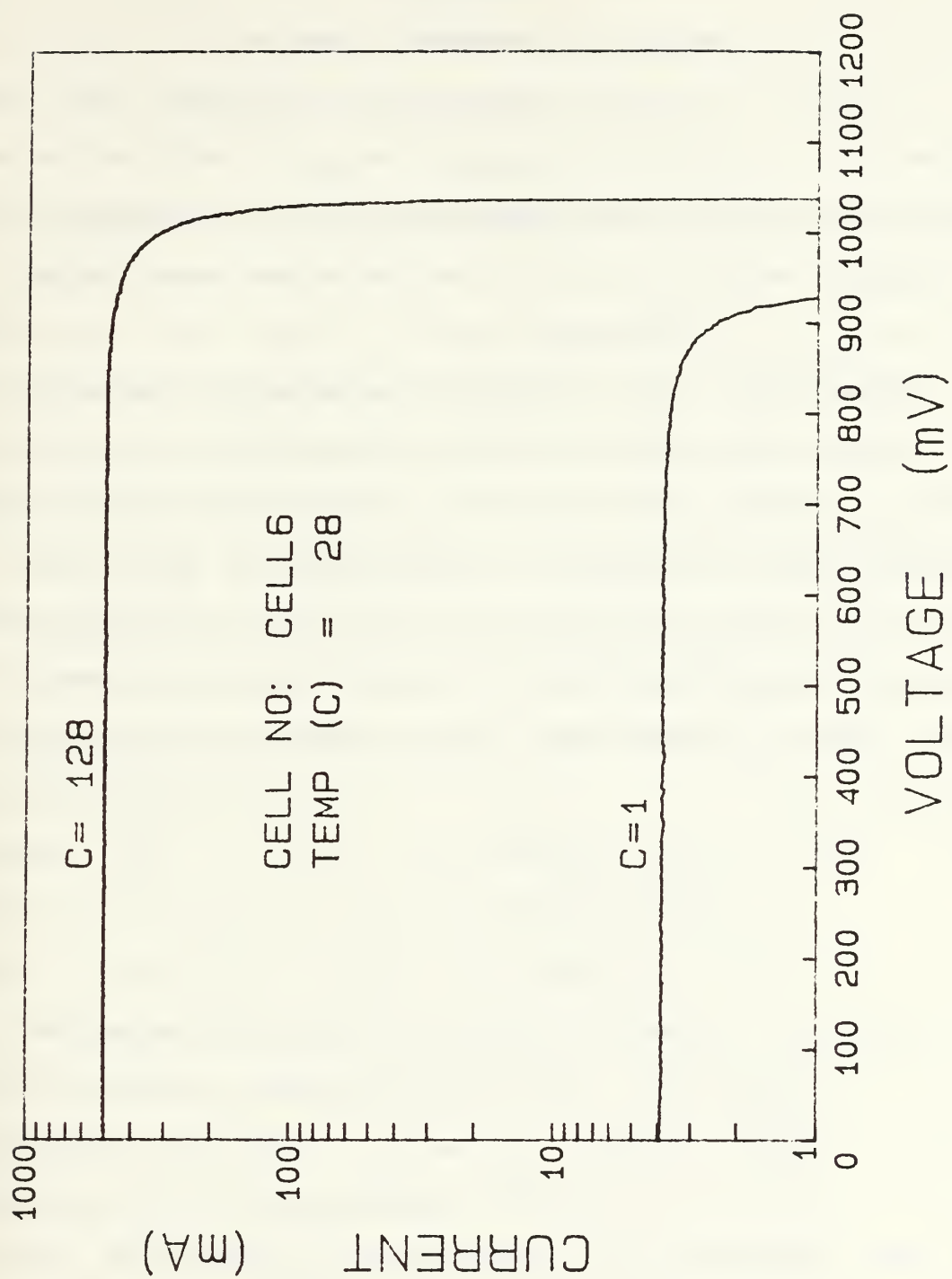


Figure 30. Comparison of Cell I-V Curves with Different Concentration Levels

APPENDIX B

SOLUTION TO DIFFERENTIAL EQUATION

In Chapter 3, it was calculated that $A_{mr} = 20.41 \text{ cm}^2$. Every concentrator has an area of A_{mr} for the optics which receives solar radiation. The radius of the projected area of the concentrator on the array surface is $r_m = 2.94 \text{ cm}$ which is calculated from Equation (17).

$$r_m^2 = A_{mr} / \pi \quad (17)$$

If the concentrators with circular mirrors are packed orthogonally, some parts of the array cannot be covered by circular mirrors because of the geometry. But the back surface area can be used totally as a radiator. Packing geometry of the mirrors is shown in Figure 31. Overall P.F. is equal to the P.F. of the unit area which is the rectangle ABCD in Figure 31. If the centers of the 4 closest circles are connected by lines, the area between these lines is the unit area (A_r). A_r can be calculated from

$$h = (4 r_m^2 - r^2)^{1/2} \quad (18)$$

$$A_r = h * 2 r_m * \cos \alpha \quad (19)$$

$$\cos \alpha = r_m / 2 r_m \quad (20)$$

The area of the 4 mirrors in this unit area is A_p . A_p is calculated

$$A_p = \pi r_m^2 (1/6 + 1/6 + 2/6 + 2/6) \quad (21)$$

$$\text{P.F.} = A_p / A_r \quad (22)$$

$$\text{P.F.} = \pi / (2 * 3^{0.5}) = 0.907 \quad (23)$$

Now, every concentrator has a radiation area of $A_r = 22.5 \text{ cm}^2$ on the back surface of the array. It is assumed the back surface of the array is coated with oil paint which has a emissivity of $\epsilon = 0.96$. The front surface

of the array is mostly covered (P.F.=0.907) by mirrors. It is assumed that the areas which are not covered with mirrors are coated with very reflective coating material ($\alpha \approx 0$, $\varepsilon \approx 0$). From Figure 31, r_n is the maximum distance between circle centers and equal to

$$r_n = r_m / \cos (\alpha/2) = 3.4 \text{ cm.} \quad (24)$$

The determination of the unknown temperature distribution within the fin requires a coupled solution. The unit radiator disk thickness is b ($=0.1\text{cm}$), inner radius is r_i ($=0.5\text{cm}$), outer radius is r_o ($=r_n$) and thermal conductivity is k . Energy is supplied to inner edge from heat pipe of radius r_i that fits the central hole and maintains the inner edge at T_i . The exposed annular surface, which is diffuse-gray with emissivity ε , radiates to the environment which at temperature $T_s = 0 \text{ K}$. The disk is thin ($b=0.1 \text{ cm}$) enough so that the local temperature can be taken as constant across the thickness b . An energy balance equates the conduction in and radiation and conduction out. The differential equation for heat transfer within the disc is

$$k \, 2\pi \, r \, b \, \frac{dT}{dr} = \varepsilon \, \sigma \, T^4 \, 2\pi \, r \, dr - k \, 2\pi \, b \, r \, \frac{dT}{dr} + (-k \, 2\pi \, r \, b \, \frac{dT}{dr}) \, dr \quad (25)$$

If b and k are constant, the energy balance becomes,

$$k \, b \, \frac{1}{r} \, \frac{d}{dr} \left(r \, \frac{dT}{dr} \right) - \varepsilon \, \sigma \, T^4 = 0 \quad (26)$$

This differential equation was solved in Siegel [Ref.: 2 pp. 390-392] for two boundary conditions $T=T_i$ at $r=r_i$ and $dT/dr=0$ at $r=r_o$. Two parameters were used (δ and γ), and Figure 32 was calculated. The equations for the parameters are

$$\gamma = (r_o - r_i)^2 \, \varepsilon \, \sigma \, T_i^3 / k \, b . \quad (27)$$

$$\delta = r_o / r_i \quad (28)$$

For copper k is equal to $4.01 \text{ W cm}^{-1} \text{ K}^{-1}$ at $T = 300 \text{ K}$. From Equation (27) and Equation (28), $\gamma^{0.5} = 0.04$ and $\delta = 6.8$ were calculated. These values give $\Omega \cong 1$ from Figure 32.

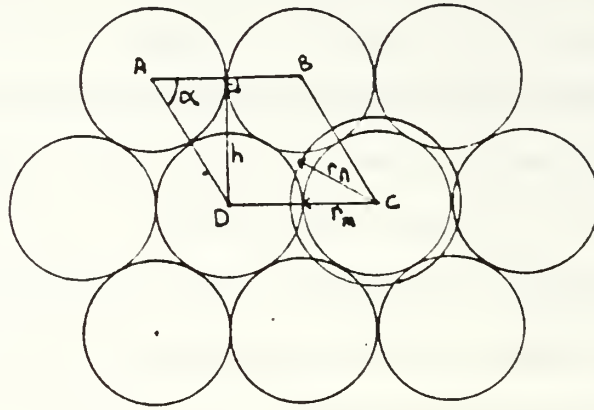
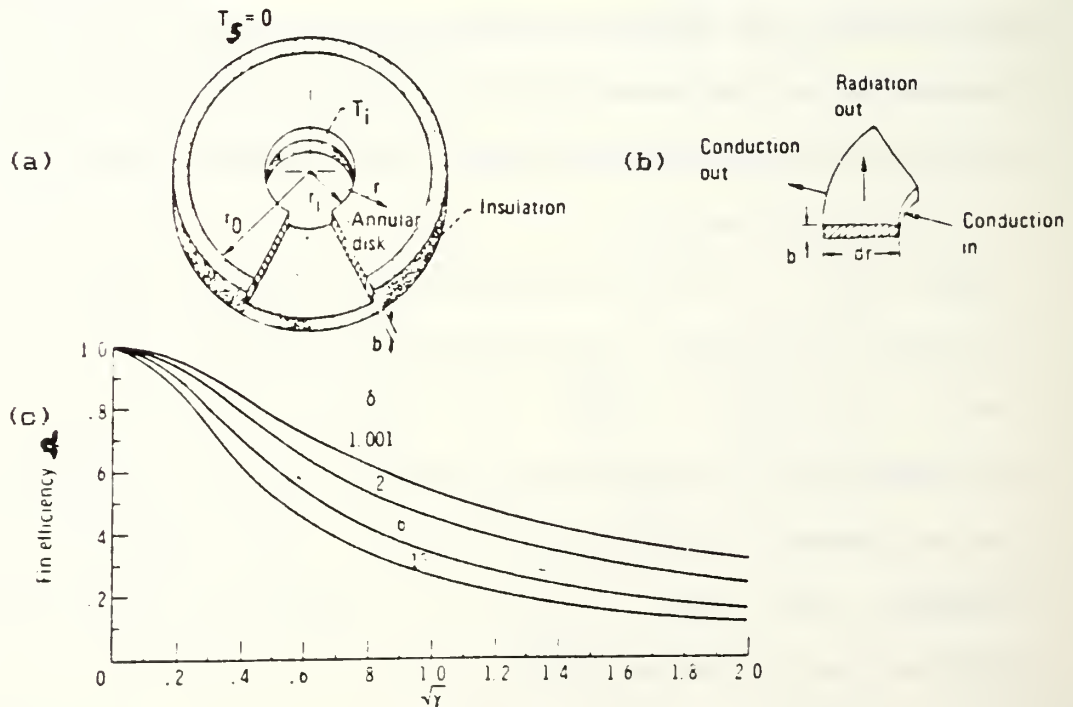


Figure 31. Orthogonal Packing of Mirrors



a) Disc Geometry b) Portion of Ring Element on Disc
c) Radiation Fin Efficiency for Disc Radiator

Figure 32. Temperature Distribution in a Thin Radiating Disc
(Reproduced from Siegel [Ref. 6:p. 390])

LIST OF REFERENCES

1. Dennis, J. F. and Brinker, D.J., GaAs and III-V Compound Solar Cells Status and Prospect for Use in Space, paper presented at the IV. European Sym. on Photovoltaic Generators in Space, 1984.
2. Gold, D.W., High Energy Electron Radiation Degredation of GaAs Solar Cells, M.S. Thesis, Naval Postgraduate School, Monterey, California, March 1986.
3. James, L.W. and Moon, R.L., "GaAs Solar Cells for Very High Concentrations," SPIE, v. 85, 1976.
4. Optics Guide 3, Melles-Griot Company, 1985.
5. Patterson, R.E., Rauschenbach, H.S., and Canrady, M.D., Design and Performance Trades for a Miniaturized Photovoltaic Concentrator Array, paper presented at the 16th IEEE Photovoltaic Specialist Conference, September 1982.
6. Siegel, R. and Howell, J.R., Thermal Radiation Heat Transfer, Hemisphere Publishing Corporation, 1981.

BIBLIOGRAPHY

Blumenberg, J., Optimization of Concentrating Solar Cell Systems with Passive and Active Cooling, ACTA Astronautica, v. II, No. 7-8, 1984.

Burges, J.W., and others, "GaAs Solar Cells for Use with Concentrated Sunlight," IEE Journal of Solid-State and Electron Devices, v. 2, June 1978.

Dunn, P.D. and D.A. Reay, Heat Pipes, Pergamon Press, 1976.

Rauschenbach, H.S., Solar Cell Array Design Handbook, Van Nostrand Reinhold Co., 1980.

Ronald, C.K., Robert Y.L., and G.S. Kamath, High-Efficiency GaAs Solar Cells, IEEE Transactions on Electron Devices, v. ED-31, No. 5, May 1984.

Shiv, C., Makoto, K., and Kiyoshi, T., "Series Resistance Effects in (GaAl)As/GaAs Concentrator Solar Cells," J. Appl. Phys., v. 50(2), February 1979.

Tada, H.Y., and others, Solar Cell Radiation Handbook, Jet Propulsion Laboratory Publication 82-69, November 1982.

INITIAL DISTRIBUTION LIST

	No.	Copies
1. Defense Technical Information Center Cameron Station Alexandria, Virginia 22304-6145	2	
2. Library, Code 0142 Naval Postgraduate School Monterey, California 93943-5002	2	
3. Distinguished Professor Allen E. Fuhs Code 72 Naval Postgraduate School Monterey, California 93943-5000	2	
4. Ltjg. Nevsan Sengil Sedat Simavi Cad., B-2 Blok, D/14 Cankaya, Ankara, Turkey	2	
5. Deniz Harbokulu Kitapligi Tuzla, Istanbul, Turkey	1	
6. Commander (Attn: SPAWAR-004-4) SPAWARSYSCOM NC-1 Washington D.C. 20363	5	
7. Naval Space Command, Code N13 Dahlgren, Virginia 22448	1	
8. Professor Sherif Michael Code 62Mi Naval Postgraduate School Monterey, California, 93943-5000	1	

DUDLEY KNOX LIBRARY
NAVAL POSTGRADUATE SCHOOL
MONTEREY, CALIFORNIA 93943-6002

Thesis
S41765 Sengil
c.1 Solar cell concentrator
system.

3 162 91

37583

Thesis
S41765 Sengil
c.1 Solar cell concentrator
system.

thesS41765

Solar cell concentrator system /



3 2768 000 71751 6

DUDLEY KNOX LIBRARY